Comparison of numerical methods for 1-D hyperbolic-type problems with free boundary

Dissertation

Comparison of numerical methods for 1-D hyperbolic-type problems with free boundary

1 次元双曲型自由境界問題の数値解法の開発と評価

Graduate School of
Natural Science and Technology
Kanazawa University

Division of Mathematical
and Physical Sciences

Course in
Computational Science

School registration No.: 1223102012
Name: Faizal Makhrus
Chief advisor: Seiro OMATA
Date of submission: July 3^{rd}, 2015

Abstract

In this research, we study a 1-D hyperbolic-type problem with free boundary. We consider a physical model that is the motion of a piece of tape being peeled off from a surface. The graph of the solution shows the shape of the tape, which displays contact angle dynamics at the free boundary (the location of peeling). Therefore, the second derivative of the solution becomes a delta function which imparts a slight difficulty. Under some assumptions, this problem can be solved numerically by the fixed domain method. Although, this method has high accuracy, it cannot be applied in some cases such as a problem where the free boundary point appears or disappears. Hence, other numerical methods are chosen for solving regularized problem, i.e., the delta function is approximated by a smoothing function. The numerical methods are: two types of finite difference methods, the finite element method, and discrete Morse flow. In this paper, the error of the regularized problem compared to the original problem is calculated. Since the choice of the parameter for smoothing function is important for the accuracy, we propose a formula to approximate the optimal parameter in order to minimize the error. This formula is verified by some experiments and we find that it can approximate the optimal parameter. In addition, based on comparisons between the numerical methods, we find that finite difference methods have better performance than the other methods.

Contents

List of Figures

Chapter 1

Introduction

In this study, we treat a physical model which can be considered as peeling tape attached to a surface. Imagine that there is a piece of tape pasted to a surface and it is peeled off from its edge smoothly. This model can be described as a stationary point of the following action integral in a suitable function space:

$$J(u) = \int_0^\tau \int_\Omega (\frac{1}{2}|\nabla u|^2 - \frac{1}{2}(u_t)^2 \chi_{u>0} + \frac{Q^2}{2}\chi_{u>0}) dx dt, \tag{1.1}$$

where u is a scalar function $(0,\tau)\times\Omega \mapsto \mathbf{R}$ which represents the shape of the tape, Q is a given positive constant, Ω is a domain in $\mathbf{R}^d (d \geq 1)$, and $\chi_{u>0}$ is a characteristic function of the set $\{(x,t) : u(x,t) > 0\}$. The following Euler-Lagrange equation can be derived from functional (1.1) under certain assumptions [2]:

$$\begin{cases} u_{tt} = \Delta u & \text{in } (\Omega \times (0,\tau)) \cap \{u > 0\}, \\ |\nabla u|^2 - (u_t)^2 = Q^2 & \text{on } (\Omega \times (0,\tau)) \cap \partial\{u > 0\}. \end{cases} \tag{1.2}$$

When $d = 1$, under certain conditions, [4] showed that the existence and the uniqueness of its solutions are obtained locally.

On the other hand, the following equation is equivalent to (1.2) (see Subsection 2.1):

$$\chi_{\{u>0\}} u_{tt} = \Delta u - \frac{Q^2}{|Du|}\mathcal{H}^d \lfloor \partial\{u > 0\} \quad \text{in } \Omega \times (0,\tau), \tag{1.3}$$

where $\mathcal{H}^d$ is d-dimensional Hausdroff measure and $Du = \left(\frac{\partial u}{\partial x_1}, \dots \frac{\partial u}{\partial x_d}, \frac{\partial u}{\partial t} \right)$. On the other hand, we consider the following equation as the approximation of problem (1.3)

$$\chi_{\{u>0\}} u_{tt} = \Delta u - \frac{Q^2}{2} (\chi^\varepsilon)'(u) \quad \text{in } \Omega \times (0, \tau), \tag{1.4}$$

where $\chi^\varepsilon(u)$ is an appropriate smoothing function. Equation (1.4) can be used to model not only the simple case of peeling tape but also more advanced free boundary problems such as water droplet attached to a plane, bubble touched the water surface, and other phenomena [3] [5] [7] [8] with constraints applied.

The motivation behind this research is to solve the original problem (1.3) yet it is difficult. Fortunately, [2] introduced the fixed domain method which solved problem (1.2) in 1D which is equivalent to the original problem (1.3) if the solution is non-negative. Fixed domain method has high accuracy. However, it is difficult to handle such model where the free boundary point appears or disappears. Therefore, we investigate another numerical methods.

We choose a few numerical methods namely:

1. explicit method 1 (spatial central difference and time forward difference)
2. explicit method 2 (spatial and time central difference)
3. finite element method (FEM)
4. discrete Morse flow (DMF).

We choose explicit method 1 and 2 as they are standard methods. Here, explicit method 2 is a standard finite difference method which can be used to analyze the error of the solution of the regularized problem. We choose FEM as it is widely used to approximate solution of hyperbolic-type problem. DMF is chosen since it is used in many hyperbolic-type problem with constraints. These methods are used to solve the regularized problem (1.4), i.e., the measure is approximated by using smoothed characteristic function. Since our motivation is to solve the original problem, we need to calculate the error of the regularized problem and this becomes the main purpose of this study (see Section 5.2).

The second purpose is to investigate how to obtain small error by the selection of the parameter of smoothed characteristic function (ε). Here, we proposed a formula to approximate the appropriate choice of ε (see Section 5.3). The third purpose is to investigate the different kinds of smoothed characteristic function. We consider two types of smoothed characteristic function and compare their influences to the accuracy of the solution in order to get the suitable one (see Section 5.4). The fourth purpose is to compare the numerical methods in order to get the suitable method (see Section 5.5). The last purpose is to implement more general case such as a model in which the free boundary points attached to a surface are more than one and they appear or vanish during simulation time (see Section 5.6).

In this dissertation, we organize our chapters as: chapter 2 explains the physical model of peeling tape, chapter 3 gives the details of fixed domain method, chapter 4 presents the numerical methods in details, chapter 5 discusses the results of our experiments, and chapter 6 gives the conclusion.

Chapter 2

Physical model of peeling tape problem

This section explains the physical model of peeling tape on a plane. Suppose there is a thin film adhered to a plane and consider this film as our tape. It is peeled off from the plane and starts to expand along the sticked tape. The region where the tape is peeled or adhered is considered as a domain Ω. We assume that the tape has the same tension γ at any places. The shape of the tape is represented by a function $u : \Omega \to \mathbf{R}$. The value of u is obtained by the stationary point of this model's energy.

There are two potential energies in this model

$$E = \int_{\{u>0\}} \gamma(\sqrt{1+|\nabla u|^2} - 1)dx + \int_{\{u>0\}} (\gamma - \sqrt{\gamma^2 + \tilde{Q}^2})dx.$$

Using Taylor expansion we can get

$$\tilde{E} = \int_{\{u>0\}} \frac{\gamma}{2}|\nabla u|^2 dx + \int_{\{u>0\}} \frac{Q^2}{2}dx,$$

where $Q^2 = \tilde{Q}^2/\gamma$. Another energy of this model is kinetic energy

$$\int_{\{u>0\}} \frac{\rho}{2}u_t^2 dx,$$

where ρ is the density of the tape per unit area. Therefore the Lagrangian

of the tape is

$$L(u,t) = \int_\Omega \left(\frac{\gamma}{2}|\nabla u|^2 - \frac{\rho}{2}u_t^2\chi_{u>0} + \frac{Q^2}{2}\chi_{u>0} \right) dx. \tag{2.1}$$

The equation of tape evolution within time interval $[0,\tau]$ is

$$J(u) = \int_0^\tau \int_\Omega \left(\frac{\gamma}{2}|\nabla u|^2 - \frac{\rho}{2}u_t^2\chi_{u>0} + \frac{Q^2}{2}\chi_{u>0} \right) dxdt. \tag{2.2}$$

We choose $\gamma = \rho = 1$.

From this energy function, the problem can be derived into Euler-Lagrange equation. Assume that the stationary point of equation (2.2) is sufficiently smooth. Let u be the stationary point of (2.2) and $u \in C^0(\Omega \times (0,\tau) \cap W^{1,2}(\Omega,\tau))$, then u satisfies

$$\Delta u - u_{tt} = 0 \ \text{ in } \{u > 0\}. \tag{2.3}$$

Moreover, if $u \in C^2(\Omega \times (0,\tau) \cap \{u > 0\})$ and $\partial\{u > 0\}$ is in C^{-1}, then u on the boundary satisfies

$$|\nabla u|^2 - u_t^2 = Q^2 \ \text{ on } \partial\{u > 0\}. \tag{2.4}$$

The proofs of (2.3) and (2.4) can be seen in [2].

The proof of (2.3) is the first variation of (2.2) with test function $\varphi \in C_0^\infty(\Omega \times (0,\tau) \cap \{u > 0\})$

$$\int_0^t \int_\Omega (\nabla u \nabla \varphi - u_t \varphi_t) dxdt = 0,$$

that is (2.3). By inner variation, we can obtain (2.4). Now, we consider $u \in C^2(\Omega \times (0,\tau) \cap \{u > 0\}$ and it is assumed that the free boundary $\partial\{u > 0\}$ belongs to C^1. For any $\eta \in C_0^\infty(\Omega \times (0,\tau); \mathbf{R}^n \times \mathbf{R})$ and $0 < \epsilon < \text{dist}(\text{spt } \eta, \partial(\Omega \times (0,\tau)))$ such that for small ϵ it follows the mapping $\psi_\epsilon : \Omega \times (0,\tau) \to \Omega \times (0,\tau)$ and we define $\psi(z) = z + \epsilon\eta(z)$. Here z is a variable of $\Omega \times \mathbf{R}$, ie. $z_j = x_j (j = 1,\ldots,n)$ and $z_{n+1} = t$. Now, let $u_\epsilon(z) = u \circ \psi^{-1}(z)$. Since u is stationary point of J it is

$$\frac{d}{d\epsilon} J(u_\epsilon)|_{\epsilon=0} = 0.$$

On the other hand, we calculate J as

$$J(u_\epsilon) = -\int_{\Omega\times(0,\tau)\cap\{u>0\}} \left\{\langle \nabla_h u(D\psi_\epsilon)^{-1}, \nabla_h u(D\psi_\epsilon)^{-1}\rangle |\det\right\} D\psi_\epsilon| dz.$$

Here, $\nabla_z f = (f_{z_1}, \ldots, f_{z_n}, f_{z_{n-1}})$ and $\nabla_h f = (f_{z_1}, \ldots, f_{z_n}, -f_{z_{n-1}})$. $\langle ., . \rangle$ is inner product of $\mathbf{R}^{n+1}$ and $D\psi_\epsilon$ is Jaccobian matrix of ψ_ϵ. Therefore,

$$\begin{aligned} J(u_\epsilon) - J(u) =& \epsilon \int_{\Omega\times(0,\tau)\cap\{u>0\}} \left\{\langle \nabla_h u, \nabla_z u\rangle + Q^2\right\} \nabla_z.\eta dz \\ & - \epsilon \int \Omega \times (0,\tau) \cap \{u>0\} 2\nabla_h u D\eta \nabla_z u dz + o(\epsilon). \end{aligned}$$

By the following equation

$$\begin{aligned} &\nabla_z.\left(\eta\langle \nabla_h u, \nabla_z u\rangle - 2\langle \eta, \nabla_z u\rangle \nabla_h u\right) \\ &= \nabla_z.\eta\langle \nabla_h u, \nabla_z u\rangle - 2\nabla_h u D\eta \nabla_z u - 2\eta\langle \eta, \nabla_z u\rangle(\Delta u - u_{tt}), \end{aligned}$$

we get

$$\begin{aligned} \frac{d}{d\epsilon} J(u_\epsilon)|_{\epsilon=0} &= \int_{\Omega\times(0,\tau)\cap\{u>0\}} \nabla_z.\left(\eta\langle \nabla_h u, \nabla_z u\rangle - 2\langle \eta, \nabla_z u\rangle \nabla_h u + Q^2\eta\right) dz \\ &= \int_{\Omega\times(0,\tau)\cap\partial\{u>0\}} \{(\langle \nabla_h u, \nabla_z u\rangle \eta - 2\langle \eta, \nabla_z u\rangle \nabla_h u).\nu \\ &\qquad + Q^2\langle \eta, \nu\rangle\} d\mathcal{H}^n. \end{aligned}$$

Here, $\mathcal{H}^n$ is n-dimensional Hausdroff measure. In addition, ν is outward unit normal vector with respect to $\Omega \times (0 \times \tau) \cap \{u > 0\}$. Since, $\nabla_z u = -\nu|\nabla_z u|$ then,

$$\frac{d}{d\epsilon} J(u_\epsilon)|_{\epsilon=0} = -\int_{\Omega\times(0,\tau)\cap\partial\{u>0\}} (\langle \nabla_h u, \nabla_z u\rangle - Q^2)\langle \eta, \nu\rangle d\mathcal{H}^n.$$

The left hand side is zero hence the free boundary condition (2.4) is obtained.

Now we consider an approximation of (2.2) where the characteristic function is approximated using a smoothed characteristic function. Firstly, we

define a smooth function called $\beta_\varepsilon(s)$. $\beta_\varepsilon(s) \in C^2(\mathbf{R})$, $\beta_\varepsilon(s) \geq 0$, and satisfies

$$\beta_\varepsilon(s) \begin{cases} = 0 & s \leq 0, \\ \leq 2/\varepsilon & 0 < s < \varepsilon \text{ and } |\beta_\varepsilon'(s)| \leq \dfrac{C}{\varepsilon^2}, \\ = 0 & \varepsilon \leq s. \end{cases}$$

It is also that $\int_0^\varepsilon \beta_\varepsilon ds = 1$ and we define B_ε

$$B_\varepsilon(u) = \int_0^u \beta_\varepsilon(s)ds \underset{\varepsilon\to 0}{\longrightarrow} \begin{cases} 1 & \text{in } \{u > 0\}, \\ 0 & \text{in } \Omega \times (0,\tau)\backslash\{u > 0\}, \end{cases}$$

which is the smoothing characteristic function of $\chi_{u>0}$.

We represent energy equation (2.2)

$$J_\varepsilon(u) = \int_0^\tau \int_\Omega \left(\frac{1}{2}|\nabla u|^2 - \chi_{u>0}\frac{1}{2}u_t^2 + \frac{Q^2}{2}B_\varepsilon(u) \right) dxdt. \tag{2.5}$$

By taking the first variation of (2.5), our problem becomes

$$\begin{cases} \Delta u - \chi_{u>0}u_{tt} = -\dfrac{Q^2}{2}\beta_\varepsilon(u) & \text{in } \Omega \times (0,\tau), \\ u(x,0) = u_0(\geq 0) \\ u_t = v_0 \\ u(x,t)|_{\partial\Omega} = f(x,t) \text{ with } f(x,0) = u_0 \text{ on } \partial\Omega. \end{cases} \tag{2.6}$$

We call this as the regularized problem.

2.1 Derivation of the original problem

In this subsection we show the derivation of (1.3) based on [6]. Let $Q_T := \Omega \times (0,\tau)$. We assume $u \in H^2(\{u > 0\}) \cap C(Q_T)$ is solution of (1.2) and satisfies $u \geq 0$ and $\{u > 0\} \subset C^{0,1}$. By definition,

$$(u_{tt} - \Delta u)(\varphi) = -\int_{Q_T} \{u_t\varphi_t - \nabla u \cdot \nabla\varphi\} dxdt, \tag{2.7}$$

here $u_{tt} - \Delta u$ is a measure. Since $u \geq 0$,

$$\begin{aligned}\left(\chi_{\overline{\{u>0\}}}u_{tt}\right)(E) &= \int_{E\cap\overline{\{u>0\}}} u_{tt} \\ &= u_{tt}\left(E\cap\overline{\{u>0\}}\right) \\ &= u_{tt}(E),\end{aligned} \tag{2.8}$$

where $E \subset Q_T$. Thus $\chi_{\overline{\{u>0\}}}u_{tt} = u_{tt}$ is in the measure sense. Then, by using above assumptions, we can calculate

$$\begin{aligned}\left(\chi_{\overline{\{u>0\}}}u_{tt} - \Delta u\right)(\varphi) &= -\int_{Q_T}\{u_t\varphi_t - \nabla u\cdot\nabla\varphi\}dxdt \\ &= \int_{\{u>0\}}(u_{tt}-\Delta u)\varphi dxdt - \int_{\partial\{u>0\}}\frac{|\nabla u|^2-(u_t)^2}{|Du|}\varphi d\mathcal{H}^m, \\ &= -\int_{\partial\{u>0\}}\frac{Q^2}{|Du|}\varphi d\mathcal{H}^m\end{aligned} \tag{2.9}$$

directly we obtain (1.3).

Chapter 3

Fixed domain method

In this section we explain fixed domain method for peeling tape model. Consider problem (1.2)

$$\begin{cases} u_{xx} - u_{tt} = 0 & \text{in } (\Omega \times (0,T)) \cap \{u > 0\}, \\ (u_x)^2 - (u_t)^2 = Q^2 & \text{on } (\Omega \times (0,T)) \cap \partial\{u > 0\}. \end{cases} \tag{3.1}$$

with initial conditions

$$\begin{cases} u(x,0) = \begin{cases} g(x) & \text{in } [0,l_0], \\ 0 & \text{otherwise,} \end{cases} \\ \\ u_t(x,0) = \begin{cases} h(x) & \text{in } [0,l_0], \\ 0 & \text{otherwise,} \end{cases} \end{cases}$$

and boundary condition

$$u(0,t) = f(t) \quad t \in (0,T),$$

where $g(x) \in C^2([0,l_0])$, $h(x) \in C^1([0,l_0])$, and $f(t) \in C^2(\mathbf{R})$,

$$\begin{cases} f(t) > 0 \quad \text{and } f'(t) \geq 0 \quad t \in (0,T), \\ g(x) > 0 \quad \text{on } [0,l_0), \\ g(0) = f(0), \quad g(l_0) = 0, \text{ and } h(0) = f'(0). \end{cases}$$

3.1 Variable change

Now, we use fixed domain method to develop the solution during $t = [0, T]$. Let y be

$$y = \frac{2x}{l(t)} - 1 \qquad x \in (0, l(t)),$$

where $l(t) = \sup\{x, u(x,t) > 0\}$ is the position of the free boundary point. We define function $\tilde{u} = \tilde{u}(y,t)$ by

$$\tilde{u}(y,t) = u(x,t) \qquad (y,t) \in (-1,1) \times (0,T) \text{ and } (x,t) \in (0,l_0) \times (0,T).$$

By changing the variable, the first equation becomes

$$\begin{aligned} 0 &= u_{xx}(x,t) - u_{tt}(x,t) \\ &= \tilde{u}_{xx}(y,t) - \tilde{u}_{tt}(y,t) \\ &= \tilde{u}_{yt}(y,t)2(y+1)\frac{l'(t)}{l(t)} - \tilde{u}_{yy}(y,t)\frac{(y+1)^2 l'(t)^2}{l(t)^2} - u_{tt} \\ &\quad + \tilde{u}_y(y,t)(y+1)\frac{l(t)l''(t) - 2l'(t)^2}{l(t)^2} + \tilde{u}_{yy}(y,t)\frac{4}{l(t)^2}. \end{aligned} \tag{3.2}$$

The second equation turns to

$$\begin{aligned} Q^2 &= u_x(l(t),t)^2 - u_t(l(t),t)^2 \\ &= \tilde{u}_x(1,t)^2 - \tilde{u}_t(1,t)^2 \\ &= \tilde{u}_y(y,t)^2\frac{4}{l(t)^2} - \tilde{u}_y(y,t)^2\left(-\frac{4l'(t)^2}{l(t)^2}\right) - \tilde{u}_t(y,t) \end{aligned} \tag{3.3}$$

$$l'(t) = \sqrt{1 - \left(\frac{Ql(t)}{2\tilde{u}_y(1,t)}\right)^2}.$$

From (3.2) and (3.3) we have

$$\begin{cases} \dfrac{\tilde{u}_{yy}(y,t)}{l(t)^2}(4-(y+1)^2 l'(t)^2) + \tilde{u}_{yt}(y,t)2(y+1)\dfrac{l'(t)}{l(t)} \\ +\tilde{u}_y(y,t)(y+1)\dfrac{l(t)l''(t)-2l'(t)^2}{l(t)^2} - u_{tt} = 0 \\ l'(t) = \sqrt{1-\left(\dfrac{Ql(t)}{2\tilde{u}_y(1,t)}\right)^2}. \end{cases} \tag{3.4}$$

The initial conditions become

$$\begin{cases} \tilde{u}(y,0) = u(x,0) = u\left(\dfrac{l_0}{2}(y+1),0\right) = g\left(\dfrac{l_0}{2}(y+1)\right) \quad y\in[-1,1], \\ \tilde{u}_t(y,0) = \tilde{u}_s(y,0) - \tilde{u}_y(y,0)\dfrac{(y+1)l'(0)}{l_0}, \\ \tilde{u}_s(y,0) = \dfrac{l'(0)}{2}(y+1)g'\left(\dfrac{l_0}{2}(y+1)\right) + e\left(\dfrac{l_0}{2}(y+1)\right). \end{cases} \tag{3.5}$$

Boundary conditions turn to

$$\left\{\tilde{u}(-1,t) = f(t), \tilde{u}(1,t) = 0, \tilde{u}_t(-1,t) = f'(t), \tilde{u}_t(1,t) = 0. \right. \tag{3.6}$$

Second derivative of l can be represented by l and l'

$$\begin{aligned} l'(t)^2 &= 1-\left(\frac{Ql(t)}{2\tilde{u}_y(1,t)}\right)^2 \quad t\in(0,T), \\ \frac{d}{dt}l'(t)^2 = 2l'(t)l''(t) &= -\frac{Q^2 l(t)(l'(t)\tilde{u}_y(1,t) - l(t)\tilde{u}_{yt}(1,t))}{2\tilde{u}_y(1,t)^3}, \\ l''(t) &= \frac{Q^2 l(t)}{4\tilde{u}_y(1,t)^3}\left(\frac{l(t)}{l'(t)}\tilde{u}_{yt}(1,t) - \tilde{u}_y(1,t)\right) \end{aligned} \tag{3.7}$$

3.2 Discretization and algorithm

Now, we divide [-1,1] into N equal intervals. The length of each partition is $\Delta y = 2/N$. Then we approximate equation (3.4) as follows

$$
\begin{cases}
\dfrac{d}{dt}u^i(t) & = v^i(t) \quad i = 1, 2, \ldots, N-1, \\
\dfrac{d}{dt}v^i(t) & = \dfrac{(4 - (y^i+1)^2 l'(t)^2)u^{i+1}(t) - 2u^i(t) + u^i(t)}{l(t)^2 \Delta y^2} \\
& \quad + 2(y^i+1)\dfrac{l'(t)(v^{i+1}(t) - v^{i-1}(t))}{2l(t)\Delta y} \\
& \quad - (y^i+1)\dfrac{(l(t)l''(t) - 2l'(t)^2)u^{i+1}(t) - u^{i-1}(t)}{2l(t)^2\Delta y} \\
& \quad i = 1, 2, \ldots, N-1, \\
l'(t) & = \sqrt{1 - \left(\dfrac{Ql(t)}{2u_y^N(t)}\right)^2}
\end{cases}
\tag{3.8}
$$

with initial conditions

$$
\begin{cases}
u^i(0) = & g\left(\dfrac{l_0}{2}(y^i+1)\right) \quad i = 1, 2, \ldots, N-1, \\
v^i(0) = & \dfrac{l'(0)}{2}(y^i+1)g'\left(\dfrac{l_0}{2}(y^i+1)\right) + e\left(\dfrac{l_0}{2}(y^i+1)\right) i = 1, 2, \ldots, N-1, \\
l'(0) = & l_0,
\end{cases}
\tag{3.9}
$$

and boundary conditions

$$
\begin{cases}
u^0(t) = & f(t), \\
u^N(t) = & 0, \\
v^0(t) = & f'(t), \\
v^N(t) = & 0,
\end{cases}
\tag{3.10}
$$

where

$$\begin{cases} l''(t) = \dfrac{Q^2 l(t)}{4(u_y^N(t))^3}\left(\dfrac{l(t)}{l'(t)}v_y^N(t) - u_y^N(t)\right), \\ u_y^N(t) = \dfrac{3u^N(t) - 4u^{N-1}(t) + u^{N-2}(t)}{2\Delta y}, \\ v_y^N(t) = \dfrac{3v^N(t) - 4v^{N-1}(t) + v^{N-2}(t)}{2\Delta y}. \end{cases} \tag{3.11}$$

We solve equation (3.8) using 4^{th} order Runge Kutta. The algorithm is presented below:

1. given initial conditions $u^i(0)$, $v^i(0)$, and $l(0)$.
2. for time $t = 0, \Delta t, \ldots, \tau$ do
   (a) set temporary variable $\tilde{u}^i = u^i(t)$, $\tilde{v}^i = v^i(t)$, and $\tilde{l} = l(t)$
   (b) for $n = 1, 2, 3, 4$
      i. $h = \Delta t$, if $n = (1, 4)$ or $h = \Delta t/2$, if $n = (2, 3)$
      ii. for $i = 1, \ldots, N$
         A. $K_n^i = v^i(t)h$
         B. $u^i(t) = \tilde{u}^i + K_n^i$
         C. $H_n^i = \dfrac{d}{dt}v^i(t)h$
         D. $v^i(t) = \tilde{v}^i + H_n^i$
      iii. $L_n = l'(t)h$
      iv. $l(t) = (\tilde{l})^i + L_n$
      v. $u_0(t) = f(t + h)$
      vi. $v_0(t) = f'(t + h)$
   (c) for $i = 1, \ldots, N$
      i. $u^i(t + \Delta t) = \tilde{u}^i + 1/6(K_1^i + 2K_2^i + 2K_3^i + K_4^i)$
      ii. $v^i(t + \Delta t) = \tilde{v}^i + 1/6(H_1^i + 2H_2^i + 2H_3^i + H_4^i)$
   (d) $l(t + \Delta t) = \tilde{l}^i + 1/6(L_1^i + 2L_2^i + 2L_3^i + L_4^i)$
   (e) $u_0(t + \Delta t) = f(t + \Delta t)$
   (f) $v_0(t + \Delta t) = f'(t + \Delta t)$

Chapter 4

Numerical methods

4.1 Explicit method 1 (spatial central difference + time forward difference)

We represent equation (1.4) using explicit method with u_{xx} approximated by central differencing. Suppose $u_t = v$ then

$$\frac{d}{dt}u_i(t) = v_i(t), \tag{4.1}$$

$$\begin{cases} \dfrac{d}{dt}v_i(t) = \dfrac{u_{i-1}(t) - 2u_i(t) + u_{i+1}(t)}{(\Delta x)^2} - \dfrac{Q^2}{2}(\chi^{\varepsilon})'(u_i(t)), & \text{if } \chi_{\{u>0\}}(x_i,t) = 1, \\ v_i(t) = 0, & \text{if } \chi_{\{u>0\}}(x_i,t) = 0, \end{cases} \tag{4.2}$$

where $i = 1, \ldots, N-1$ and

$$\chi_{\{u>0\}}(x_i,t) = \begin{cases} 1 & \text{if } \max(u_{i-1}u_i, u_{i+1}) > 0, \\ 0 & \text{otherwise.} \end{cases}$$

The initial and boundary conditions are $u(0,t) = f(t)$, $u(x,0) = g(x)$, $u_t(0,t) = f'(t)$, and $u_t(x,0) = h(x)$. We solve (4.1)-(4.2) using the 4th order Runge-Kutta. The algorithm is presented below

1. given initial condition $u^i(0)$ and $v^i(0)$.
2. for time $t = 0, \Delta t, \ldots, \tau$ do

(a) set temporary variable $\tilde{u}^i = u^i(t)$ and $\tilde{v}^i = v^i(t)$

(b) for $n = 1, 2, 3, 4$

i. $h = \Delta t$, if $n = (1, 4)$ or $h = \Delta t/2$, if $n = (2, 3)$

ii. for $i = 1, \ldots, N-1$

A. $K_n^i = v^i(t)h$

B. $u^i(t) = \tilde{u}^i + K_n^i$

C. $H_n^i = \dfrac{d}{dt}v^i(t)h$

D. if $(\max(u^{i-1}, u^i, u^{i+1}) > 0)$ then $v^i(t) = \tilde{v}^i + H_n^i$

E. else $v^i(t) = 0$

iii. $u_0(t) = f(t + h)$

iv. $v_0(t) = f'(t + h)$

(c) for $i = 1, \ldots, N-1$

i. $u^i(t + \Delta t) = \tilde{u}^i + 1/6(K_1^i + 2K_2^i + 2K_3^i + K_4^i)$

ii. $v^i(t + \Delta t) = \tilde{v}^i + 1/6(H_1^i + 2H_2^i + 2H_3^i + H_4^i)$

(d) $u_0(t + \Delta t) = f(t + \Delta t)$

(e) $v_0(t + \Delta t) = f'(t + \Delta t)$

4.2 Explicit method 2 (spatial and time central difference)

This method utilizes a standard finite difference discretization. We approximate u_{xx} and u_{tt} from equation (1.4) using centered differencing. Here, $[0, \tau]$ is divided by M equal intervals, $0 = t_0 < t_1 < \ldots < t_M = \tau$.

$$\chi_{\{u>0\}}(x_i, t_k)\frac{u_i^{k+1} - 2u_i^k + u_i^{k-1}}{(\Delta t)^2} = \frac{u_{i+1}^k - 2u_i^k + u_{i-1}^k}{(\Delta x)^2} - \frac{Q^2}{2}(\chi^\varepsilon)'(u_i^k), \quad (4.3)$$
$$i = 1, \ldots, N-1, \quad \text{and} \quad k = 1, \ldots, M-1,$$

where $u_i^k = u(x_i, t_k)$. Then we calculate the solutions using the following

$$\begin{cases} u_i^{k+1} & = 2u_i^k - u_i^{k-1} + (\Delta t)^2 \left(\dfrac{u_{i+1}^k - 2u_i^k + u_{i-1}^k}{(\Delta x)^2} - \dfrac{Q^2}{2}(\chi^\varepsilon)'(u_i^k) \right), \\ & \quad \text{if } \chi_{\{u>0\}}(x_i, t_k) = 1, \\ u_i^{k+1} & = 0, \\ & \quad \text{if } \chi_{\{u>0\}}(x_i, t_k) = 0. \end{cases} \tag{4.4}$$

The boundary conditions are $u(0,t) = f(t)$, $u(x,0) = g(x)$, and $u_t(x,0) = h(x)$.

4.3 Finite Element Method

To implement finite element method, we multiply equation (1.4) by any test function $\xi \in C_0^\infty(\Omega)$ and integrate over the space domain

$$\int_\Omega (\chi_{\{u>0\}} u_{tt} - u_{xx} + \frac{Q^2}{2}(\chi^\varepsilon)'(u))\xi dx = 0.$$

By integration by parts we obtain

$$\int_\Omega (\chi_{\{u>0\}} u_{tt}\xi + u_x\xi_x + \frac{Q^2}{2}(\chi^\varepsilon)'(u)\xi)dx = 0, \quad \forall \xi \in C_0^\infty(\Omega). \tag{4.5}$$

We divide Ω into N intervals and find the approximate solution of (4.5) in the set

$V_t = \{u \in C^0(\bar{\Omega})\colon u|_{\partial\Omega} = f(\cdot, t),\ u \text{ is linear on every } [x_{k-1}, x_k],\ k = 1, \ldots, N\}$

for each time $t \in (0, \tau)$, where $f : \bar{\Omega} \times [0, \tau]$ is a given function. Then the approximate solution can be described by $u(x,t) = \sum_{i=0}^N a_i(t)\varphi_i(x)$, where

$$\varphi_i(x) = \left(1 - \frac{|x - x_i|}{\Delta x}\right)_+, \quad i = 0, \ldots, N.$$

Here the symbol $(\ )_+$ implies $(\ f(x)\ )_+ = \max(f(x), 0)$. We substitute the approximate solution u to (4.5)

$$\int_\Omega \left(\chi_{\{u>0\}} \sum_{i=0}^N a_i''\varphi_i\xi + \sum_{i=0}^N a_i\varphi_i'\xi' + \frac{Q^2}{2}(\chi^\varepsilon)' \sum_{i=0}^N a_i\varphi_i\xi \right) dx = r, \ \forall \xi \in C_0^\infty(\Omega), \tag{4.6}$$

where r is the residual which comes from the approximated representation of function u. We choose φ_j, $j = 1, \ldots, N-1$, as our test function and rewrite (4.6) as follows:

$$\sum_{i=0}^{N}\left[a_i''\int_\Omega \chi_{\{u>0\}}\varphi_i\varphi_j dx\right] + \sum_{i=0}^{N}\left[a_i\int_\Omega \varphi_i'\varphi_j' dx\right] + \frac{Q^2}{2}\int_\Omega (\chi^\varepsilon)'\sum_{i=0}^{N} a_i\varphi_i\varphi_j dx = 0,$$
$$\text{j} = 1,2,\ldots,\ \text{N-1}.$$

This can be written in vector form

$$Ba'' + Aa + \frac{Q^2}{2}C(a) = p,$$

where a is the column vector with entries $a_1, \ldots, a_{N-1}$,

$$A = \frac{1}{\Delta x}\begin{bmatrix} 2 & -1 & 0 & 0 & 0 & \cdots & 0 & 0 \\ -1 & 2 & -1 & 0 & 0 & \cdots & 0 & 0 \\ 0 & -1 & 2 & -1 & 0 & \cdots & 0 & 0 \\ \vdots & \vdots & \vdots & \vdots & \vdots & \vdots & \ddots & \vdots \\ 0 & 0 & 0 & 0 & 0 & \cdots & -1 & 2 \end{bmatrix}$$

and

$$B = \frac{\Delta x}{6}\begin{bmatrix} 4\tilde{\chi}(a_1) & \tilde{\chi}(a_1) & 0 & 0 & 0 & \cdots & 0 & 0 \\ \tilde{\chi}(a_2) & 4\tilde{\chi}(a_2) & \tilde{\chi}(a_2) & 0 & 0 & \cdots & 0 & 0 \\ 0 & \tilde{\chi}(a_3) & 4\tilde{\chi}(a_3) & \tilde{\chi}(a_3) & 0 & \cdots & 0 & 0 \\ \vdots & \vdots & \vdots & \vdots & \vdots & \vdots & \ddots & \vdots \\ 0 & 0 & 0 & 0 & 0 & \cdots & \tilde{\chi}(a_{N-1}) & 4\tilde{\chi}(a_{N-1}) \end{bmatrix}.$$

Here, $\tilde{\chi}(a_i) = 1$, whenever $\max(a_{i-1}, a_i, a_{i+1})$ is greater than zero and $\tilde{\chi}(a_i) = 0$ otherwise. Here, C is a column vector whose elements are determined by a and p is determined by boundary values.

We approximate a'' using central difference with $a_i^k = a_i(t_k)$ and $a^k = (a_1^k, \ldots, a_{n-1}^k)$:

$$B\frac{a^{k+1} - 2a^k + a^{k-1}}{(\Delta t)^2} + Aa^k + \frac{Q^2}{2}C(a^k) = p.$$

The final form is

$$Ba^{k+1} = 2Ba^k - Ba^{k-1} - (\Delta t)^2\left(Aa^k + \frac{Q^2}{2}C(a^k) - p\right). \qquad (4.7)$$

We define $a_i^{k+1} = 0$, if $b_{ii} = 0$ where b_{ii} is the diagonal element of matrix B at i^{th} row. In general, matrix B is non-symmetric. We can change the position of the known value of a_i^{k+1} to the right hand side and adjust the matrix B to be a symmetric matrix. Now, we approximate the solution a^{k+1} of (4.7) by conjugate gradient method. The algorithm is written below

1. Given initial conditions $a_0^0,\ a_0^1$, and a_0^2 which are column matrix. We also choose ω as a small number.

2. For time $[n\Delta t, \tau],\ n = 2, \ldots, M$ do the following

   (a) Set $flag = 0$ and $k = 0$

   (b) while $flag = 0$

      i. calculate column matrix $b = 2Ba_k^{n-1} - Ba_k^{n-2} - (\Delta t)^2 \left(Aa_k^{n-1} + \frac{Q^2}{2} C(a_k^{n-1}) + p \right)$

      ii. calculate column matrix $o = Ba_k^n$

      iii. calculate decent gradient $\nabla f_k(a_k^n) = b - o$, if $k = 0$, or $\nabla f(a_k^n) = \nabla f(a_k^n) + \beta_{k-1} \nabla f(a_{k-1}^n)$, if $k > 0$,
      where $\beta_{k-1} = \dfrac{-\nabla f(a_k^n)^T B \nabla f(a_{k-1}^n)}{\nabla f(a_{k-1}^n)^T B \nabla f(a_{k-1}^n)}$

      iv. if $|\nabla f(a_k^n)| < \omega$ set $flag = 1$

      v. calculate the stepsize $\alpha = \dfrac{\nabla f(a_k^n).\nabla f(a_k^n)}{\nabla f(a_k^n) B \nabla f(a_k^n)}$

      vi. $a_{k+1}^n = a^n + \alpha \nabla f(a_k^n)$ and set $k = k + 1$;

   (c) $a_0^{n+1} = a_{k+1}^n$. a_0^{n+1} is the solution at $t = (n+1)\Delta t$

4.4 Discrete Morse Flow

Let us consider problem (1.4) with u^0 as the initial value, v^0 as the initial velocity and $u^1 = u^0 + \Delta t v^0$. Now, we determine the time step $\Delta t = \tau/M$, where $M > 0$ is a natural number. Then, the approximate solution for the next time $t = k\Delta t$, $k = 2, 3, \ldots, M$ is defined by the minimizer $u^k \in \mathcal{K}$ of

$$J_k(u) = \int_\Omega \frac{|u - 2u^{k-1} + u^{k-2}|^2}{2(\Delta t)^2} \chi_{\{u>0\}} dx + \frac{1}{2} \int_\Omega |\nabla u|^2 dx + \frac{Q^2}{2} \int_\Omega \chi^\varepsilon(u) dx,$$

where $u^j(x) = u(x, t_j)$, $t_j = j\Delta t$ $(j = k-2, k-1)$ and $\mathcal{K} = \{u \in \mathbf{W}^{1,2}(\Omega); u = g \text{ on } \partial\Omega\}$.

We approximate u^k as a piecewise linear function, so that the functional's values are approximated:

$$J_k(u) \approx \sum_{i=1}^{N} \int_{x_{i-1}}^{x_i} \left(\frac{|u - 2u^{k-1} + u^{k-2}|^2}{2(\Delta t)^2} \chi_{\{u>0\}} + \frac{1}{2}|\nabla u|^2 + \frac{Q^2}{2}\chi^{\varepsilon}(u) \right) dx. \tag{4.8}$$

We calculate the first term as follows:

$$\begin{aligned} &\int_{x_{i-1}}^{x_i} \frac{|u - 2u^{k-1} + u^{k-2}|^2}{2(\Delta t)^2} \chi_{\{u>0\}} dx \\ &= \begin{cases} (v^2 + w^2 + vw)\dfrac{\Delta x}{6(\Delta t)^2} & u_{i-1} > 0,\ u_i > 0, \\ (w^2 + (v_2)^2 + wv_2)\dfrac{x_c - x_i}{6(\Delta t)^2} & u_{i-1} \le 0,\ u_i > 0, \\ ((w_2)^2 + v^2 + w_2 v)\dfrac{x_c - x_{i-1}}{6(\Delta t)^2} & u_{i-1} > 0,\ u_i \le 0, \\ 0 & \text{otherwise}, \end{cases} \end{aligned}$$

where $v = |u_{i-1} - 2u_{i-1}^{k-1} + u_{i-1}^{k-2}|$, $w = |u_i - 2u_i^{k-1} + u_i^{k-2}|$, $u_{i-1} = u(x_{i-1}, t)$, $u_i = u(x_i, t)$, $v_2 = v - \dfrac{w - v}{u_i - u_{i-1}} u_{i-1}$, $w_2 = v_2$ and $x_c = x_{i-1} - \dfrac{\Delta x}{u_i - u_{i-1}} u_{i-1}$. The second term is

$$\frac{1}{2}\int_{x_{i-1}}^{x_i} |\nabla u_i|^2 dx = \frac{(u_{i+1} - u_i)^2}{2\Delta x},$$

and for the third term we have

$$\int_{x_{i-1}}^{x_i} \chi^{\varepsilon}(u)dx$$

$$= \begin{cases} \Delta x & u_{\max} \geq \varepsilon,\ u_{\min} \geq \varepsilon, \\ 1 - \dfrac{\Delta x}{u_{\min} - u_{\max}} \left(\dfrac{-u_{\min}(u_{\min} - \varepsilon)}{2\varepsilon} - (\varepsilon - u_{\max}) \right) & u_{\max} \geq \varepsilon,\ 0 \leq u_{\min} < \varepsilon, \\ \dfrac{u_{\max}\Delta x}{2(u_{\max} - u_{\min})} & u_{\max} \geq \varepsilon,\ u_{\min} \leq 0, \\ \dfrac{\Delta x}{2\varepsilon}(u_{\max} + u_{\min}) & 0 \leq u_{\max} < \varepsilon,\ 0 \leq u_{\min} < \varepsilon, \\ \dfrac{u_{\max}^2 \Delta x}{2\varepsilon(u_{\max} - u_{\min})} & 0 \leq u_{\max} < \varepsilon,\ u_{\min} \leq 0, \\ 0 & \text{otherwise}, \end{cases}$$

where $u_{\max} = \max(u_{i-1}, u_i)$ and $u_{\min} = \min(u_{i-1}, u_i)$. We find the minimizer of (4.8) using a non-linear conjugate gradient method. The algorithm is as below

1. Given initial condition $u_0,\ u_1$, and u_2 as our initial guess. We choose ω as a small number.
2. For time $[n\Delta t, \tau],\ n = 2, \ldots, M$ do the following
   (a) $a_0 = u_n$
   (b) Set $flag = 0$ and $k = 0$
   (c) while $flag = 0$
      i. If $k = 0$ compute gradient $g_k = \nabla J_n(a_k)$
      ii. Find $\alpha_k = \arg\min_{\alpha}\ J_n(a_k - \alpha g_k)$.
      iii. $a_{k+1} = a_k - \alpha_k g_k$
      iv. set $k = k + 1$
      v. apply Polak-Ribiere formula to compute β_k

$$\beta_k = \frac{\nabla J_n(a_k).(\nabla J_n(a_k) - \nabla J_n(a_{k-1}))}{|\nabla J_n(a_{k-1})|^2}$$

      vi. Compute conjugate direction $g_k = \beta_k \nabla J_n(a_{k-1}) - \nabla J_n(a_k)$
      vii. if $|\nabla J_n(a_k)| < \omega$ then $flag = 1$
   (d) $u_n = a_k$

Chapter 5

Numerical results

In this chapter, we explain our experiments and results. There are two problems in our experiments which we need to compare. The first problem is

$$\begin{cases} u_{tt} = u_{xx}, & \text{in } (\Omega \times (0,\tau)) \cap \{u > 0\} \\ (u_x)^2 - (u_t)^2 = Q^2, & \text{on } (\Omega \times (0,\tau)) \cap \partial\{u > 0\} \\ u(0,t) = f(t), & \\ u(x,0) = g(x), & \\ u_t(x,0) = h(x), & \end{cases} \tag{5.1}$$

approximated by fixed domain method. The second is

$$\begin{cases} \chi_{\{u>0\}} u_{tt} = u_{xx} - \dfrac{Q^2}{2}(\chi^\varepsilon)'(u), & \text{in } (\Omega \times (0,\tau)) \\ u(0,t) = f(t), & \\ u(x,0) = g(x), & \\ u_t(x,0) = h(x), & \end{cases} \tag{5.2}$$

approximated by two types of finite different method, FEM, and DMF. The initial conditions of our experiments are

$$\begin{aligned} l_0 =& \frac{1}{\sqrt{Q^2 + f'(0)^2}} \\ g(x) =& \max(1 - \frac{1}{l_0}x, 0), \\ h(x) =& \begin{cases} f'(0) & 0 < x \le l_0, \\ 0 & l_0 < x, \end{cases} \end{aligned}$$

and $f(t)$ are

Case 1 Peeling speed is constant $f(t) = at + 1$. The exact solution of this case is $u(x,t) = \max(1 + t - \frac{1}{l_0}x, 0)$.

Case 2 Peeling speed is increasing $f(t) = (at + 1)^2$.

Case 3 Peeling speed is decreasing $f(t) = \sqrt{at + 1}$.

Case 4 Peeling speed is stopping at some times $f(t) = 1 + at + \sin\ t$

Case 5 Peeling direction is downward (pasting the tape).

$$\begin{aligned} g(x) =& \max(10 - \frac{1}{l_0}x, 0), \\ f(t) =& 10 - at, \\ h(x) =& \begin{cases} f'(0) & 0 < x \le l_0, \\ 0 & l_0 < x, \end{cases} \end{aligned}$$

Case 6 Peeling directions are upward and downward (oscillating tape) $f(t) = 1 + 0.3 \sin\ t$.

Let us introduce some notation. The space domain Ω is divided into N intervals, $x_0 < x_1 < \ldots < x_N$, then the characteristic function is smoothed as follows

$$(\chi^\varepsilon)'(u) = \begin{cases} 1/\varepsilon & 0 < u < \varepsilon, \\ 0 & \text{otherwise.} \end{cases} \tag{5.3}$$

Next, the characteristic function is

$$\chi_{\{u>0\}}(x_i,t) = \begin{cases} 1 & \text{if } \max\left(u(x_{i-1},t), u(x_i,t), u(x_{i+1},t)\right) > 0, \\ 0 & \text{otherwise,} \end{cases} \tag{5.4}$$

At last, since we are interested in observing the biggest error of the solutions during time t, we define the error of numerical solutions

$$E_u = \max_{\substack{i=0,\dots,N \\ k=0,\dots,M}} |u^*(x_i,t_k) - u_i^k|, \tag{5.5}$$

where u^* is the exact solution or fixed domain method solution and u_i^k is numerical solution at x_i in time t_k.

5.1 Exact solution of the approximated problem

We construct the exact solution of (1.4) for a special case. Let $\Omega = \mathbf{R}$, then we describe problem (1.4) as

$$\chi_{\{u>0\}} u_{tt} = \Delta u - \frac{Q^2}{2}(\chi)'(u) \quad \text{in } \mathbf{R} \times (0,\tau). \tag{5.6}$$

Here $u^\varepsilon : (0,\tau) \times \mathbf{R} \mapsto \mathbf{R}$ is the exact solution of (5.6) and we assume that u^ε is

$$u^\varepsilon(x,t) = F(z) \qquad z = x - vt,$$

where v is a constant and $0 < v < 1$, $F : \mathbf{R} \to \mathbf{R}$; $F(0) = 0$, $F'(0) = 0$, $F \in C^1(\mathbf{R})$. This solution can be considered as peeling tape with a constant peeling speed where the solution is increasing but keeps its shape as shown in 5.1. Therefore we get

$$\chi_{\{F>0\}} v^2 F''(z) = F''(z) - \frac{Q^2}{2}(\chi^\varepsilon)'(F). \tag{5.7}$$

Then, we separate F into three intervals: $\{F > \varepsilon\}$ where the solution F is a linear function, $\{0 < F \le \varepsilon\}$ where the solution F is quadratic function, and $\{F = 0\}$. We assume that the free boundary point position is at $z_0 (F(z_0) = 0)$ and $F(z_\varepsilon) = \varepsilon$ as shown in figure 5.1. Then we can construct the exact solution as follows

- if $z \in \{F = 0\}$ therefore $F(z) = 0$.

- if $z \in \{0 < F \leq \varepsilon\}$ then

$$\begin{aligned} v^2 F''(z) &= F''(z) - \frac{Q^2}{2\varepsilon}, \\ (1 - v^2) F''(z) &= \frac{Q^2}{2\varepsilon}, \\ F''(z) &= \frac{Q^2}{2\varepsilon(1 - v^2)}, \\ F'(z) &= \frac{Q^2}{2\varepsilon(1 - v^2)} z, \\ F(z) &= \frac{Q^2}{4\varepsilon(1 - v^2)} z^2, \end{aligned} \tag{5.8}$$

- if $z \in \{F > \varepsilon\}$, using

$$\begin{aligned} \varepsilon &= \frac{Q^2}{4\varepsilon(1 - v^2)} z_\varepsilon^2, \\ z_\varepsilon &= -\frac{2\varepsilon\sqrt{1 - v^2}}{Q}. \end{aligned}$$

$F(z)$ in this interval is

$$\begin{aligned} F(z) &= F'(z_\varepsilon)(z - z_\varepsilon) + \varepsilon, \\ &= -\frac{Q^2}{2\varepsilon(1 - v^2)} \frac{2\varepsilon\sqrt{1 - v^2}}{Q} (z - z_\varepsilon) + \varepsilon, \\ &= -\frac{Q}{\sqrt{1 - v^2)}} (z - z_\varepsilon) + \varepsilon. \end{aligned} \tag{5.9}$$

We summarize as follow

$$F(z) = \begin{cases} -\dfrac{Q}{\sqrt{1-v^2}}(z - z_\varepsilon) + \varepsilon & z < z_\varepsilon, \\ \dfrac{Q^2}{4\varepsilon(1-v^2)}z^2 & z_\varepsilon \le z < z_0, \\ 0, & z_0 \le z. \end{cases} \tag{5.10}$$

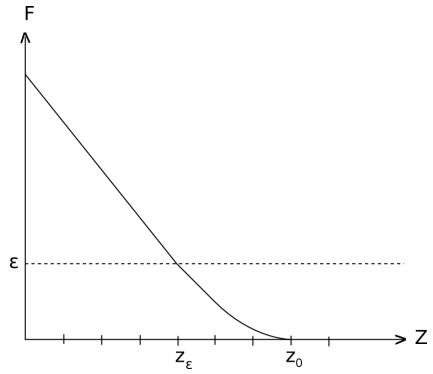

Figure 5.1: Exact solution (5.7)

5.2 Error in the peeling tape model using smoothed characteristic functions

We solve cases 1-6 using explicit method 2 and compare with the exact solution for case 1 and fixed domain method solutions for cases 2-6. The parameters are shown in table 5.1

	Q^2	Ω	a	Δt	Δx
explicit method 2	1	[0,15]	1	$0.9\Delta x$	varied
fixed domain method	1	[-1,1]	1	0.0005625	0.002

Table 5.1: Parameters for explicit method 2 and fixed domain method

The comparisons are shown in figure 5.3. From the figures, we can see that the errors of solutions from all cases tend to be small when Δx is decreasing

with ε. They show that small and big ε give large error and so we analyze this error pattern. Since the precise error is difficult to find, we only approximate it. Here, the error of the explicit method 2 satisfies the inequality

$$\max_{\substack{i=0,\dots,N\\k=0,\dots,M}} |u^*(x_i,t_k) - u_i^k| \le E_1 + E_2 \tag{5.11}$$

where

$$E_1 = \max_{\substack{i=0,\dots,N\\k=0,\dots,M}} |u^*(x_i,t_k) - u^\varepsilon(x_i,t_k)|, \qquad E_2 = \max_{\substack{i=0,\dots,N\\k=0,\dots,M}} |u^\varepsilon(x_i,t_k) - u_i^k|,$$

and u^* is the exact solution of problem (1.2), u^ε is the exact solution of (1.4), and u is the solution of (4.4). From this inequality we expect to obtain the error pattern.

We calculate the error of finite difference (explicit method 2). We define

$$\begin{aligned} e_i^k =& \frac{u^\varepsilon(x_i,t_{k-1}) - 2u^\varepsilon(x_i,t_k) + u^\varepsilon(x_i,t_{k+1})}{\Delta t^2} \\ & - \frac{u^\varepsilon(x_{i-1},t_k) - 2u^\varepsilon(x_i,t_k) + u^\varepsilon(x_{i+1},t_k)}{\Delta x^2} + \frac{Q^2}{2}(\chi^\varepsilon)'(u^\varepsilon(x_i,tk)) \end{aligned} \tag{5.12}$$

and subtract (5.12) from (5.6)

$$\begin{aligned} u_{tt}^\varepsilon - u_{xx}^\varepsilon + \frac{Q^2}{2}(\chi^\varepsilon)'(u^\varepsilon) =& \frac{u^\varepsilon(x_i,t_{k-1}) - 2u^\varepsilon(x_i,t_k) + u^\varepsilon(x_i,t_{k+1})}{\Delta t^2} \\ & - \frac{u^\varepsilon(x_{i-1},t_k) - 2u^\varepsilon(x_i,t_k) + u^\varepsilon(x_{i+1},t_k)}{\Delta x^2} \\ & + \frac{Q^2}{2}(\chi^\varepsilon)'(u^\varepsilon(x_i,tk)) - e_i^k. \end{aligned}$$

Since the error occurs near to z_0 and z_ε at first we calculate for z_0 ($x_i - vt_k = 0$)

$$\begin{aligned} e_i^k =& \frac{\{F(v\Delta t) - 2F(0) + F(-v\Delta t)\}}{\Delta t^2} - u_{tt} \\ & - \frac{\{F(-\Delta x) - 2F(0) + F(\Delta x)\}}{\Delta x^2} + u_{xx}. \end{aligned}$$

We want to find the upper bound of the error

$$\begin{aligned}\left|e_i^k\right| &\leq \left|\frac{\{F(v\Delta t) - 2F(0) + F(-v\Delta t)\}}{\Delta t^2} - u_{tt}\right| \\ &\quad + \left|-\frac{\{F(-\Delta x) - 2F(0) + F(\Delta x)\}}{\Delta x^2} + u_{xx}\right| \\ &\leq \left|\frac{-Q^2v^2}{4\varepsilon(1-v^2)}\right| + \left|\frac{Q^2}{4\varepsilon(1-v^2)}\right|.\end{aligned}$$

Since $0 < v < 1$ then we have

$$\left|e_i^k\right| \leq \frac{Q^2}{2\varepsilon(1-v^2)}. \tag{5.13}$$

In the same way, we can get $\left|e_i^k\right|$ for z_ε which is also $\dfrac{Q^2}{2\varepsilon(1-v^2)}$. Since $|e_i^k|$ is the error of finite differencing, we expect

$$E_2 \sim \frac{g_u^2 \Delta x}{2\varepsilon}, \tag{5.14}$$

where g_u is the gradient of the solution and $g_u^2 = \dfrac{Q^2}{1-v^2}$. In this experiment we can consider g_u is a constant C.

Next, we assume the error $E_1 = \tilde{C}\varepsilon$. Therefore the total error is

$$\max_{i=0,\ldots,N} |u^*(x_i, t_k) - u_i^k| \leq \tilde{C}\varepsilon + \frac{C\Delta x}{\varepsilon}. \tag{5.15}$$

The graph of this total error can be seen in figure 5.2. In this figure, there are two Δx: 0.01 and 0.005. When Δx decreases, the error also decreases for particular ε. It also shows that when ε is big or small, the error increases. This is approximately similar to the error pattern in figure 5.3a and serves to justify our results.

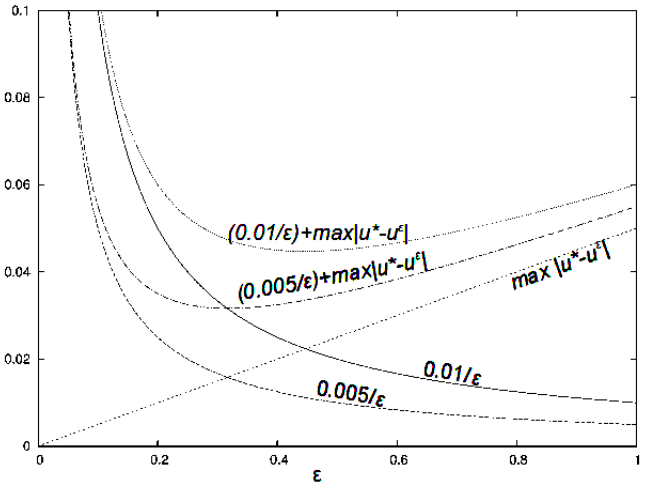

Figure 5.2: Estimation from above of the total error for explicit method 2

5.3 Comparisons of solution having different gradient

We are also interested in investigating the choice of ε to get optimal error related to the gradient of the solution near the free boundary point (g_u). The relation between g_u and the error is shown in (5.14). The gradient of the solution is approximated by calculating the linear regression of five u_i whose values are nearest to the value 0.1. This value is chosen since, based on figure 5.3a-5.3d, when $\varepsilon = 0.1$, they display similar errors for different Δx.

To see the relation between the error of the solutions and g_u, we conduct a few experiments using cases 1-4 with different g_u. We choose only cases 1-4 since they are enough to represent different kinds of solutions. We set the gradient of the solution at time $\tau = 7$ to be 1 to 40. The results are shown in figures 5.5 and 5.6. Figure 5.5 shows that the range of optimal ε becomes larger when g_u increases. In addition, the figure 5.6 shows that there are two surfaces. The lower surfaces describe the lower bound of the range for the optimal ε. While the upper surfaces describe the upper bound of the range for the optimal ε. From the figure, the range of the optimal ε becomes large if the gradient of the solution increases.

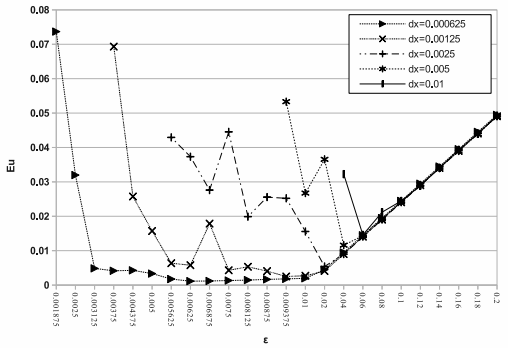

(a) E_u case 1 at time level τ=9

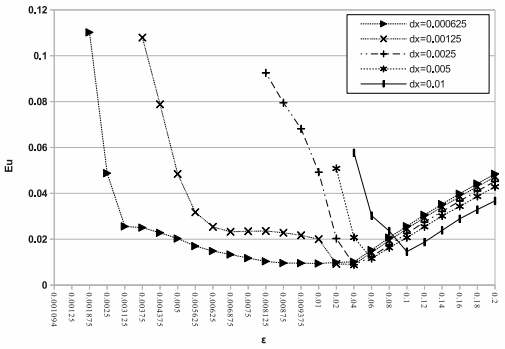

(b) E_u case 2 at time level τ=9

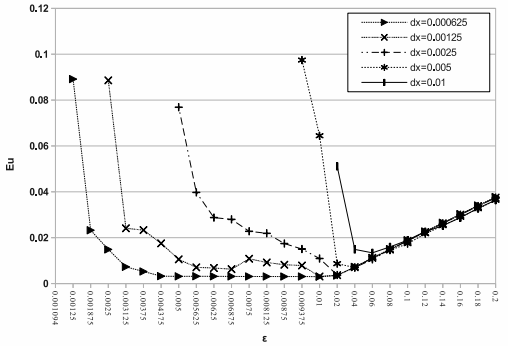

(c) E_u case 3 at time level τ=9

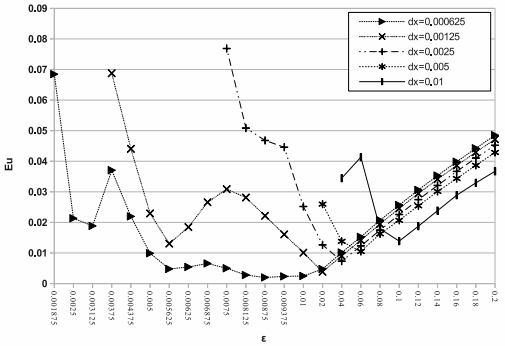

(d) E_u case 4 at time level τ=9

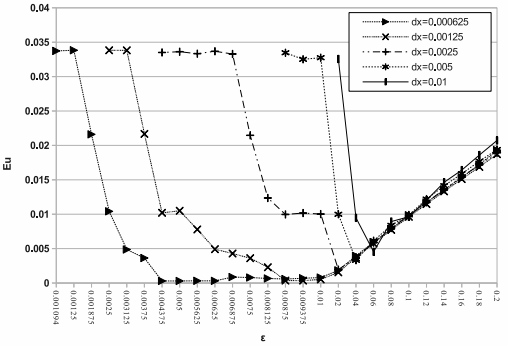

(e) E_u case 5 at time level τ=9

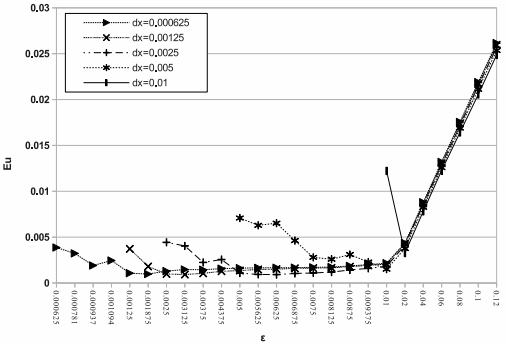

(f) E_u case 6 at time level τ=7

Figure 5.3: The errors of explicit method 2 for cases 1-6

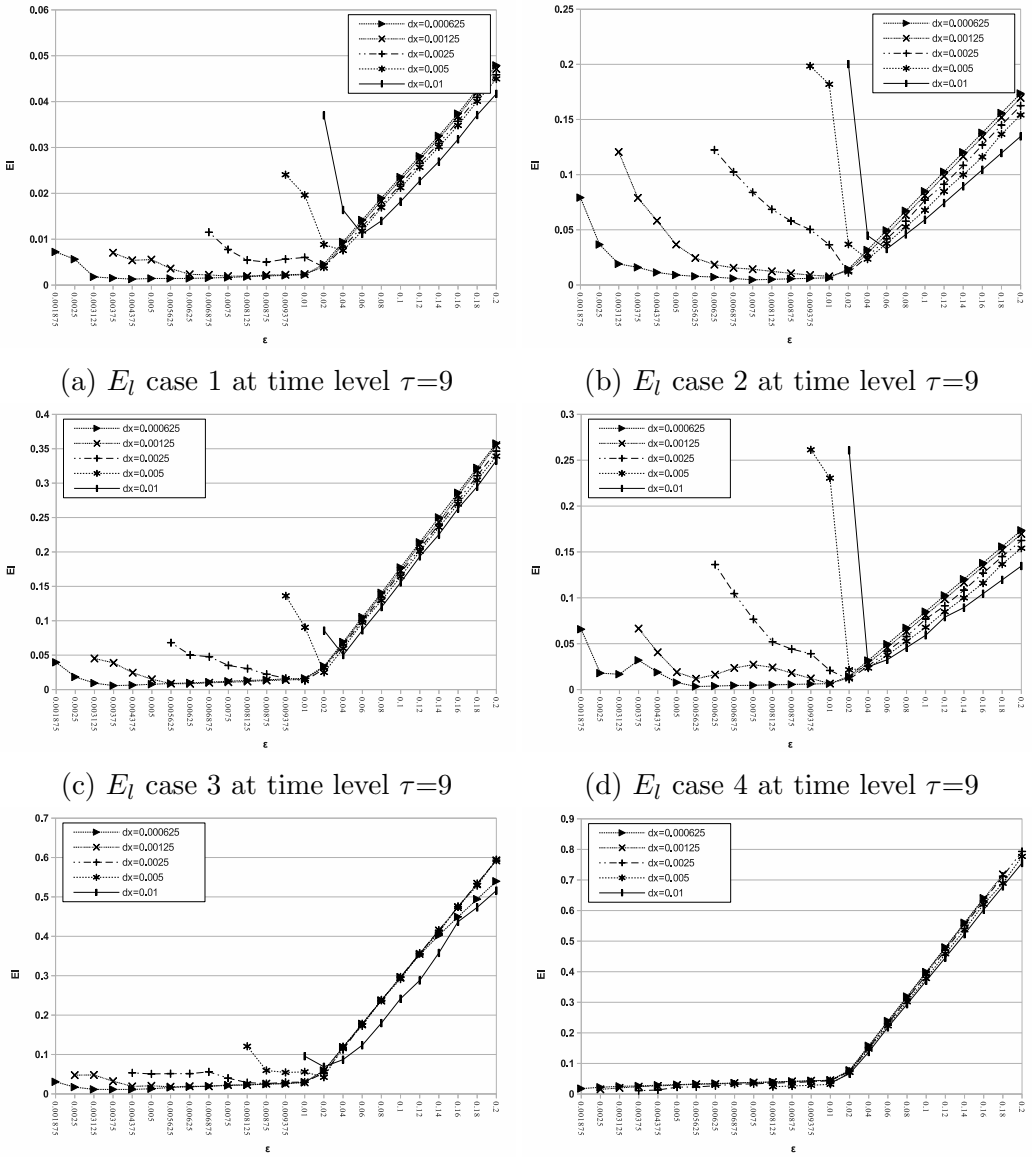

(a) E_l case 1 at time level τ=9

(b) E_l case 2 at time level τ=9

(c) E_l case 3 at time level τ=9

(d) E_l case 4 at time level τ=9

(e) E_l case 5 at time level τ=9

(f) E_l case 6 at time level τ=7

Figure 5.4: The errors of free boundary point of cases 1-6

The optimal ε can be derived from (5.15)

$$\varepsilon = Cg_u\sqrt{\Delta x}. \tag{5.16}$$

From the experiments above, the range of constant C in (5.16) is shown in

figure 5.7. In this figure, each vertical line indicates the range of constant C which applies for the gradient 1 to 40 using specific Δx. It shows when the constant C is between 0.15-0.16, it satisfies for all cases and Δx. Therefore, we conclude that the constant C is approximately 0.15-0.16.

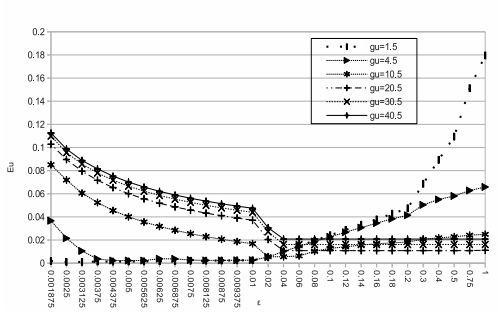

(a) the error of solution for case 1

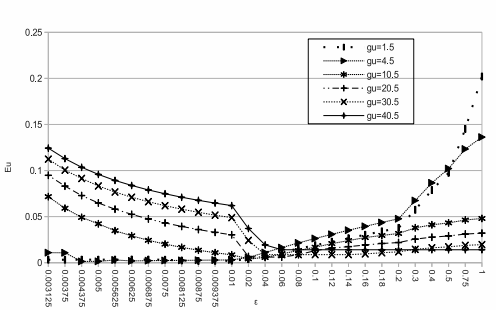

(b) the error of solution for case 2

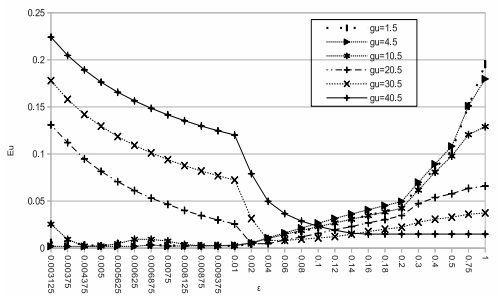

(c) the error of solution for case 3

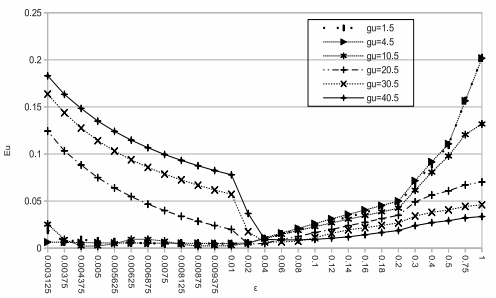

(d) the error of solution for case 4

Figure 5.5: The errors of solution for case 1-4 with different gradient with $\Delta x = 0.000625$

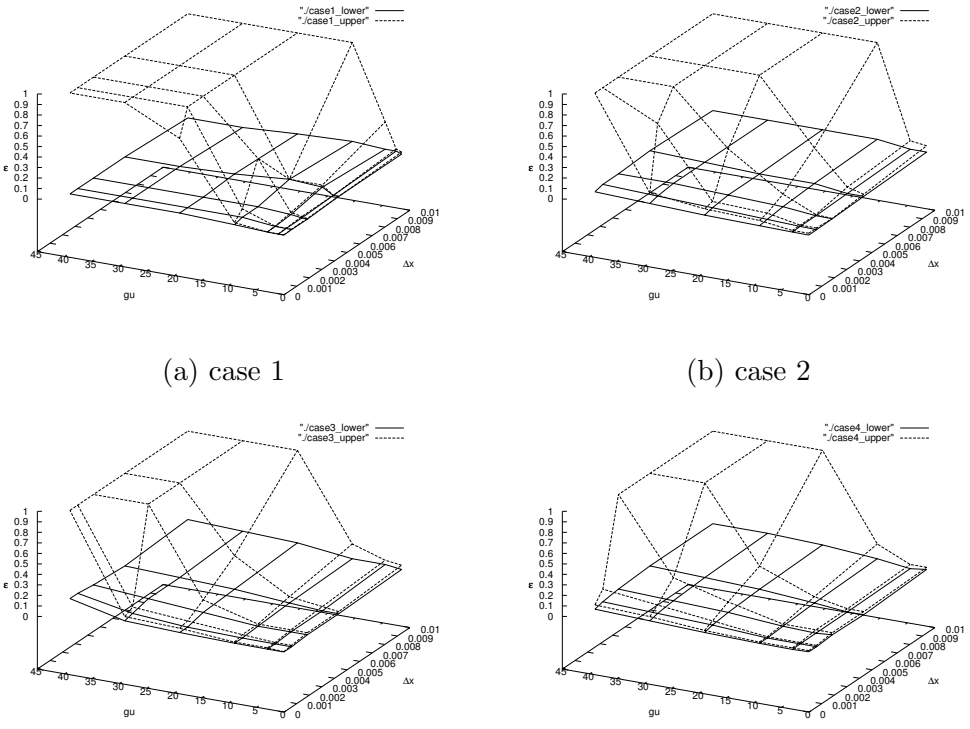

(a) case 1

(b) case 2

(c) case 3

(d) case 4

Figure 5.6: the lower and upper bound of optimal ε for cases 1-4

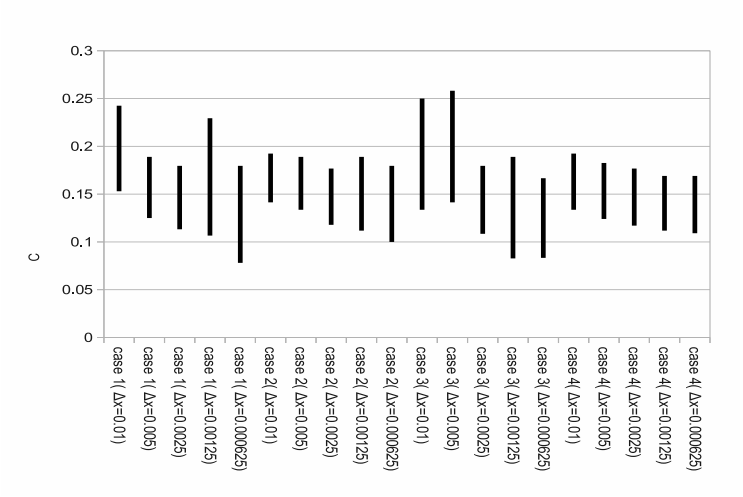

Figure 5.7: The range of constant C for cases 1-4 with different Δx

5.4 Comparisons of smoothing characteristic functions

In this experiment, we compare two smoothed characteristic functions. In particular, (5.3) and

$$(\chi^{\varepsilon})'(u) = \begin{cases} \dfrac{hu}{a} & 0 < u < a, \\ h & a \le u \le \varepsilon - a, \\ \dfrac{h(\varepsilon - u)}{a} & \varepsilon - a \le u \le \varepsilon, \\ 0 & \text{otherwise}, \end{cases} \tag{5.17}$$

where

$$a = \frac{\varepsilon}{b}, \qquad h = \frac{1}{\varepsilon - a},$$

b is a positive number. Function (5.17) has a smoother transition than (5.3). We want to know whether smooth transitions influence the accuracy. The goal of this experiment is to get the appropriate smoothed characteristic function.

We apply these two functions in equation (1.4) with parameters $Q^2 = 1,\ \Omega = [0, 15],\ a = 1,\ \Delta x = 0.005,$ and $\Delta t = 0.9\Delta x$ and solve using explicit

method 2. The errors of each cases at time level $\tau = 9$ (case 6 uses $\tau = 7$) are shown in figure 5.8. The errors are calculated by

$$\tilde{E}_u = \max_{\substack{i=0,\dots,N \\ k=0,\dots,M}} |u_i^*(x_i, t_k) - (u^{(5.3)})_i^k| \quad \text{or} \quad \tilde{E}_u = \max_{\substack{i=0,\dots,N \\ k=0,\dots,M}} |u_i^*(x_i, t_k) - (u^{(5.17)})_i^k|, \tag{5.18}$$

where $u^{(5.3)}$ and $u^{(5.17)}$ are solutions with smoothed characteristic function (5.3) and (5.17) respectively. In this figure, we can see that the errors of solutions using smoothed characteristic function (5.3) and (5.17) for cases 1-6 are relatively same with an order of $10^{-3} - 10^{-4}$. Therefore, (5.3) is an adequate smoothed characteristic function.

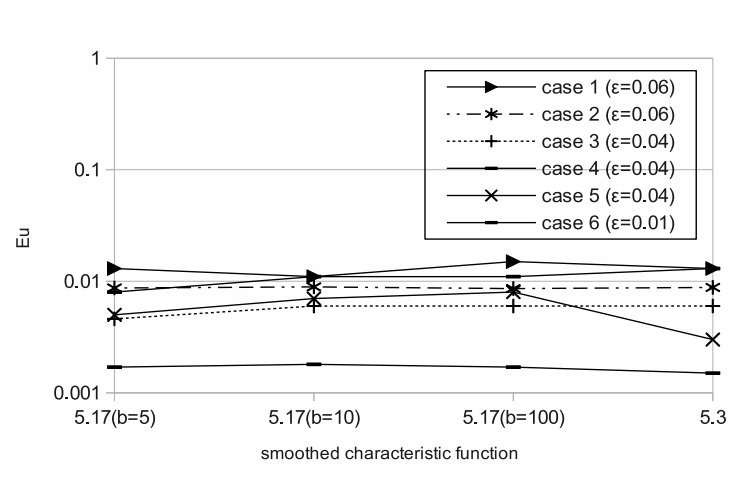

Figure 5.8: Comparison of smoothed characteristic functions

5.5 Comparisons of numerical methods

To compare numerical methods, we conduct two experiments. The first experiment is to numerically solve (5.7) and compare the results with the exact solution (5.10). In order to do this, we consider a case similar to case 1 with

initial conditions

$$u^{\varepsilon}(x,0) = \begin{cases} -\dfrac{1}{l_0}x + 1 & 0 \le x \le l_0 - \varepsilon l_0, \\ \dfrac{(x - l_0 - \varepsilon l_0)^2}{4\varepsilon (l_0)^2} & l_0 - \varepsilon l_0 \le x \le l_0 + \varepsilon l_0, \\ 0 & l_0 + \varepsilon l_0 \le x, \end{cases}$$

$$u^{\varepsilon}(0,t) = \sqrt{\frac{1}{(l_0)^2} - Q^2}\ t + 1,$$

$$u_t^{\varepsilon}(x,0) = \begin{cases} \sqrt{\dfrac{1}{(l_0)^2} - Q^2} & 0 \le x \le l_0 - \varepsilon l_0, \\ \dfrac{\sqrt{\dfrac{1}{(l_0)^2} - Q^2}}{2\varepsilon l_0}(x - l_0 - \varepsilon l_0) & l_0 - \varepsilon l_0 \le x \le l_0 + \varepsilon l_0, \\ 0 & l_0 + \varepsilon l_0 \le x. \end{cases}$$

The exact solution is $u^{\varepsilon}(x,t) = F(x - l_0 - (\varepsilon/a) - \sqrt{1 - (Q/a)^2}\ t)$. We choose the parameters $Q^2 = 1,\ \Omega = [0, 15],\ \Delta x = 0.005$ and Δt as in Table 5.2 below.

explicit method 1	explicit method 2	FEM	DMF
0.0045	0.0045	0.0025	0.0005

Table 5.2: Δt for numerical methods

The error is calculated by

$$C_u = \max_{\substack{i=0,\ldots,N \\ k=0,\ldots,M}} |u^{\varepsilon}(x_i, t_k) - u_i^k|,$$

and figure 5.9 shows the errors. In this figure, The errors C_u of all methods decrease when ε is bigger. It means that the numerical solutions become similar to the exact solution of approximated problem when ε is big. In addition, explicit method 2 has the smallest error

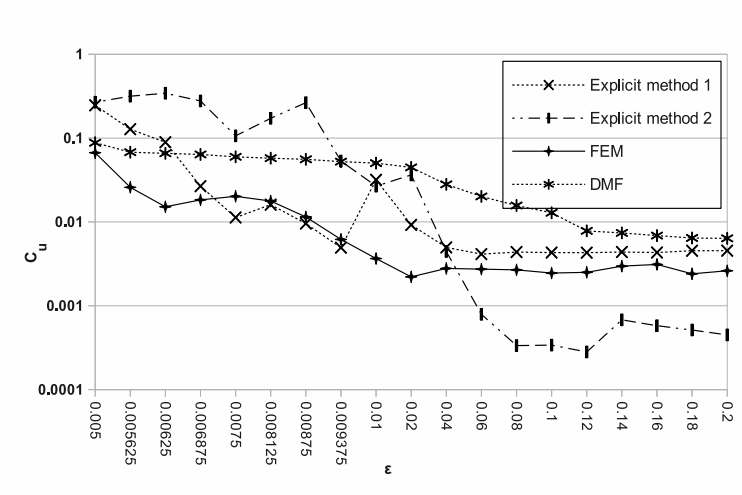

Figure 5.9: Error of numerical methods and exact solution of equation (5.7)

The second experiment applies numerical methods to above cases 1-6 and compares the errors of each methods. We choose the parameters $Q^2 = 1,\ \Omega = [0, 15],\ \Delta x = 0.005,\ \varepsilon = 0.04$ and Δt as in table 5.2. The errors of the methods are shown in table 5.3. From this table, the error differences of each method are in the order $10^{-3} - 10^{-4}$.

Now, we conduct comparisons using several ε for cases 1-4. Figure 5.10 shows the results. In this figure, the errors of each method are relatively similar in the order 10^{-4}. Therefore, we conclude that all methods have similar accuracy. In addition, the computation time of each method can be seen in table 5.4. Based on the computation time, DMF is slow due to its algorithm and the requirement of small Δt. We try several Δt and find that when $\Delta t \leq 0.1\Delta x$ the errors of DMF solution approach the errors of other methods. On the other hand, DMF has advantage that it can include additional constraints such as volume constraint to support advanced models like droplet motion. Hence, this method is appropriate to be used further. Regarding the FEM approach, we find that $\Delta t \leq 1/2\Delta x$ gives stable solutions.

case	explicit method 1	explicit method 2	FEM	DMF
1	0.008	0.011	0.01	0.0097
2	0.02	0.02	0.023	0.012
3	0.0079	0.006	0.0075	0.0074
4	0.013	0.013	0.014	0.0097
5	0.005	0.003	0.005	0.006
6	0.007	0.008	0.007	0.009

Table 5.3: E_u at time $\tau = 9$ (cases 1-5) and $\tau = 7$ (case 6)

method	time
fixed domain method	2s
explicit method 1	3s
explicit method 2	3s
FEM	6s
DMF	>15mins

Table 5.4: Time complexity

Δt	E_u
$1 \times \Delta x$	0.09
$0.75 \times \Delta x$	0.05
$0.5 \times \Delta x$	0.03
$0.25 \times \Delta x$	0.009
$0.1 \times \Delta x$	0.007

Table 5.5: Comparison of Δt for DMF method on case 1 with $\varepsilon = 0.02$

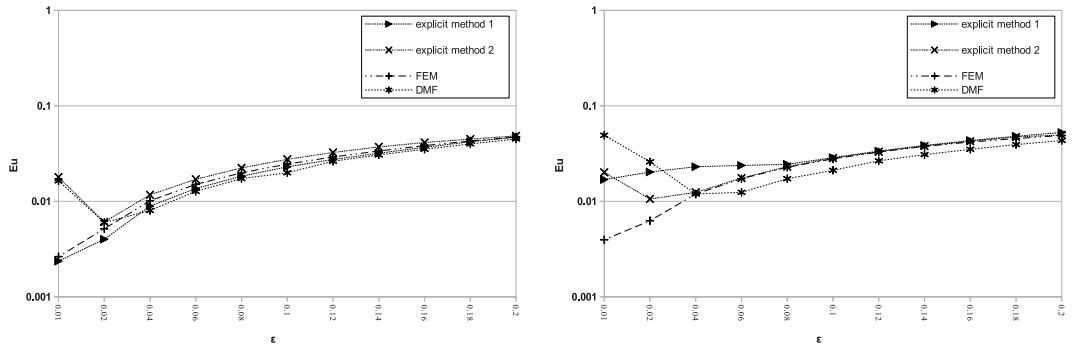

(a) E_u case 1

(b) E_u case 2

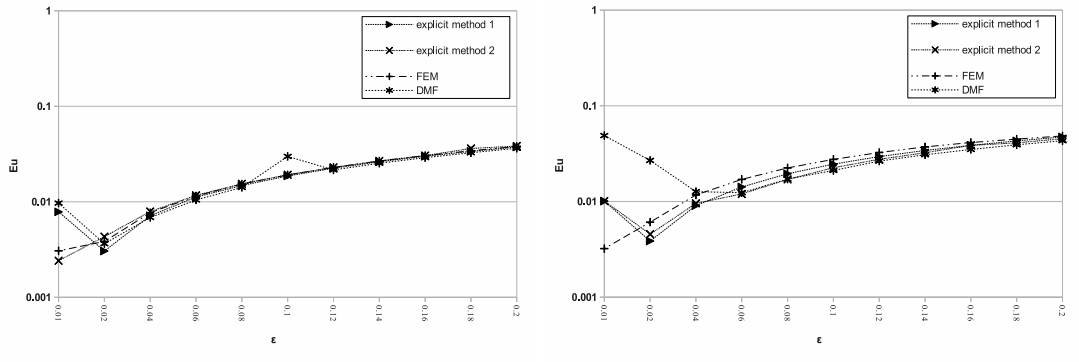

(c) E_u case 3

(d) E_u case 4

Figure 5.10: E_u at $\tau = 9$ of cases 1-4

5.6 Advanced cases

Now, we implement more advanced cases where the free boundary points are more than one and they emerge or vanish during time t. We choose $\Omega = [0, 2]$ (except case 7) , $Q^2 = 1$, $\Delta x = 0.005$, Δt as shown in table 5.2 and initial conditions are listed below

case 7 peeling tape from two sides

We modify case 1 above by peeling off from the beginning and end of the tape. Our domain is $\Omega = [0, 5]$. The peeling velocities at both sides are the same as case 1. The tape is peeled off until the free boundaries vanish and from here it becomes a wave equation. Since case 1 has an exact solution, it can be used to obtain the exact solution of the wave

equation using d'Alembert's formula. In this case, we only consider the exact solution in the middle point of Ω.

To get the exact solution of the wave equation at $x = 2.5$, we first consider the exact solution of case 1,

$$g(x,t) = \max(1 + t - \frac{1}{l_0}x, 0)$$

and its velocity $h(x,t)$. The time that the free boundary disappears is $t = 2.535$. From this time on, the solution evolves by the wave equation: we define $t_{wave} = t - 2.535$ and the exact solution is

$$\begin{aligned} u(2.5, t_{wave}) =& 0.5(g(2.5 + t_{wave}, 2.535) + g(2.5 - t_{wave}, 2.535) + \\ & \int_{2.5-t_{wave}}^{2.5+t_{wave}} h(2.5, 2.535)dx). \end{aligned}$$

We only use the exact solution in the mid point $x = 2.5$.

case 8 pulling down a string from the middle

$$u(x,0) = 0.5,\ u_t(x,0) = -20x(2-x),\ u(0,t) = u(2,t) = 0.5$$

case 9 an unstable curve

$$u(x,0) = \max(-0.8(2x-2)^6 + 2(2x-2)^4 - 2.2(2x-2)^2 + 1, 0)$$

$$u_t(x,0) = 0,\ u(0,t) = u(2,t) = 0$$

case 10 collision of four waves

$$u(x,t) = \sum_{i=1}^{4} \max(-6(x - a_i - t)^2 + 0.16, 0),$$

where $a_i = a_{i-1} + 0.37$ and $a_0 = 6$.

The solutions of above cases are shown in figure 5.11-5.14.

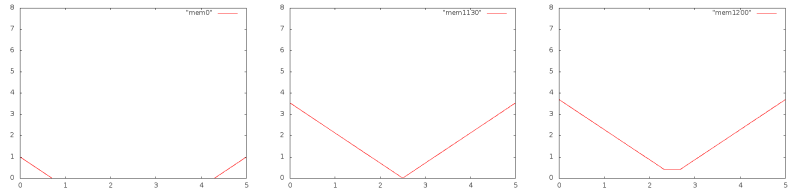

(a) $t = 0$ (b) $t = 2.825$ (c) $t = 3$

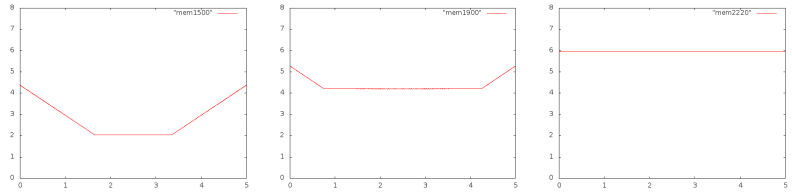

(d) $t = 3.75$ (e) $t = 4.75$ (f) $t = 5$

Figure 5.11: The numerical solutions of case 7

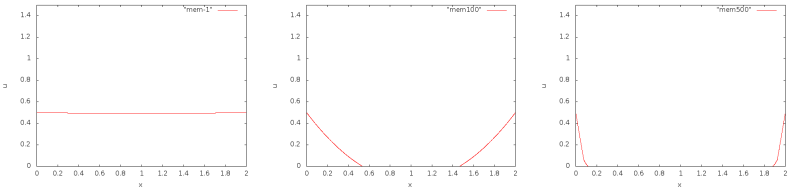

(a) $t = 0$ (b) $t = 0.016$ (c) $t = 0.032$

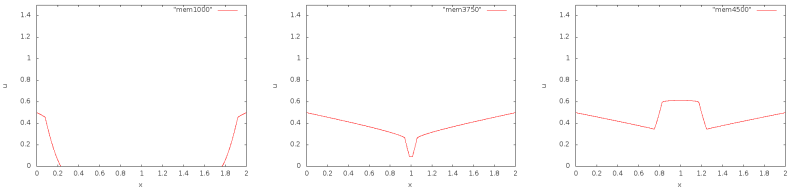

(d) $t = 0.16$ (e) $t = 1.17$ (f) $t = 1.4$

Figure 5.12: The numerical solutions of case 8

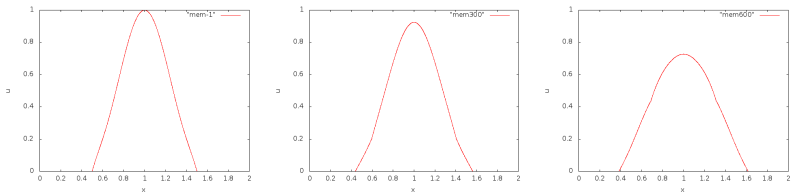

(a) $t = 0$ (b) $t = 0.093$ (c) $t = 0.018$

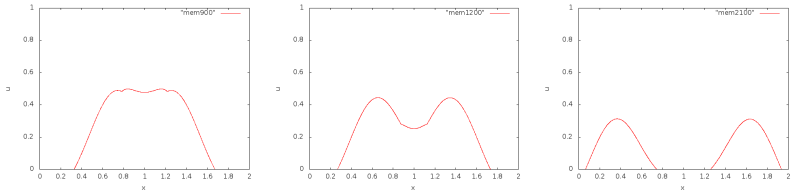

(d) $t = 0.28$ (e) $t = 0.375$ (f) $t = 0.65$

Figure 5.13: The numerical solutions of case 9

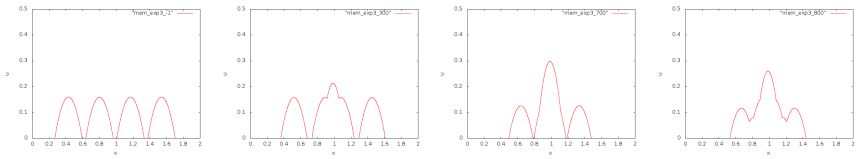

(a) $t = 0$ (b) $t = 0.093$ (c) $t = 0.22$ (d) $t = 0.25$

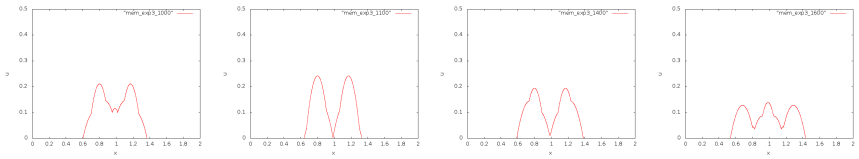

(e) $t = 0.31$ (f) $t = 0.34$ (g) $t = 0.43$ (h) $t = 0.5$

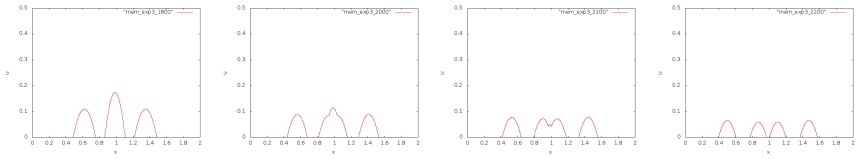

(i) $t = 0.56$ (j) $t = 0.625$ (k) $t = 0.65$ (l) $t = 0.69$

Figure 5.14: The numerical solutions of case 10

For case 7, we compare the solution of the mid point when the free boundaries vanish with the exact solution by $E = |u^*(2.5, t) - u(2.5, t)|$. We choose $\varepsilon = 0.04$. The result can be seen in figure 5.15. The error is of the same order as the error of case 1 (see 5.3a). Therefore, we conclude that our numerical methods can handle the case where the free boundary appears or vanishes with relatively small error (10^{-2})

For cases 8-10, as we do not have the exact solutions, we calculate the differences between explicit method 1, FEM, and DMF with explicit method 2. We calculate the differences by

$$D_u = \max_{\substack{i=0,\dots,N \\ k=0,\dots,M}} |(u^{ex2})_i^k - u_i^k|$$

where u^{ex2} is solution of explicit method 2 and u_i is the solution of explicit method 1, FEM, or, DMF at $x = i$. The comparison is shown in table 5.6. From table 5.6 we see that the differences of the solutions are of order 10^{-3}. Hence we can say that all methods are relatively similar.

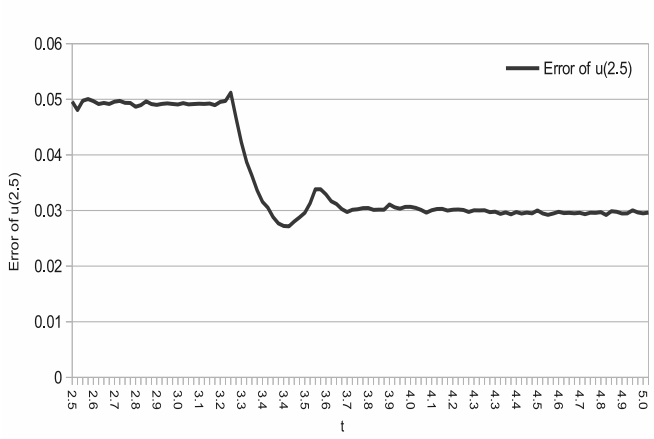

Figure 5.15: Error in case 7 at $u(2.5, 5)$

case	t	explicit method 1	FEM	DMF
7	0.2	0.0023	0.0008	0.0038
8	0.6	0.0061	0.0014	0.0017
9	0.5	0.0032	0.0016	0.0025

Table 5.6: D_u of numerical methods

We summarize the features of the numerical methods in table 5.8 below

	Fixed domain method	Explicit method 1	Explicit method 2	FEM	DMF
accuracy	10^{-11}	10^{-3}	10^{-3}	10^{-3}	10^{-3}
stability	$\Delta t \leq 0.1\Delta x$	$\Delta t = 0.9\Delta x$	$\Delta t = 0.9\Delta x$	$\Delta t \leq 0.5\Delta x$	$\Delta t \leq 0.1\Delta x$
easy to implement	medium	medium	easy	medium	hard
computation time	fast	fast	fast	fast	slow
free boundary appear and disappear	no	yes	yes	yes	yes

Table 5.8: The features of numerical methods

From the table we conclude: first, the accuracy of fixed domain method is the highest compared to the other methods. Second, DMF requires small Δt (at least $\leq 0.1\Delta x$) to be stable which makes this method becoming slow. Third, the computation time of DMF is long since the minimization process needs many iterations. Fourth, only fixed domain method which can not handle the appearance and disappearance of the free boundary point.

Chapter 6

Conclusion

We solved a one dimensional hyperbolic-type problem with free boundary and a smoothed characteristic function by finite difference method (explicit method 2) and compared with exact or fixed domain method solutions. From experiments 1 and 2, we obtained the error pattern of explicit method 2 and confirmed using approximation that this error pattern holds. From this pattern, it shows that there are optimal ε which minimize the error. Therefore we proposed a formula to calculate the optimal ε with respect to the gradient of the solution and Δx. This formula includes a constant which, based on experiment, we found to be within 0.15 to 0.16 for gradients with values in 1 to 40. In experiment 3, we conclude that the smooth transitions in the smoothed characteristic function does not impart a large influence in accuracy and that (5.3) is an adequate smoothed characteristic function. In experiments 4 and 5, we compared four numerical methods solving the peeling tape problem and more advanced cases and found that explicit method 1 and 2 have good performance.

Appendix A

Finite element method

We will change this equation into matrix form

$$\sum_{i=0}^{N}\left[(a_i)_{tt}\int_\Omega \chi_{\{u>0\}}\varphi_i\varphi_j dx\right]+\sum_{i=0}^{N}\left[(a_i)\int_\Omega (\varphi_x)_i(\varphi_x)_j dx\right]$$
$$+\frac{Q^2}{2}\int_\Omega (\chi^\varepsilon)'(\sum_{i=0}^{N}a_i\varphi_i)\varphi_j dx=0$$
$$j=1,2,\ldots,N-1$$

We change the first term if $i=j$

$$\begin{aligned}\int_{x_{i-1}}^{x_{i+1}}\chi_{\{u>0\}}\varphi_i\varphi_j dx &= 2\int_{x_{i-1}}^{x_{i+1}}\chi_{\{u>0\}}(u(x))\frac{1}{\Delta x^2}(x-x_{i-1})^2dx\\ &=\frac{2}{\Delta x^2}\int_{x_{i-1}}^{x_{i+1}}\tilde{\chi}(a_i)(x-(i-1)\Delta x)^2dx\\ &=\frac{2}{\Delta x^2}\left[\tilde{\chi}(a_i)\frac{1}{3}(x-x_{i-1})^3\right]_0^{\Delta x}\\ &=\tilde{\chi}(a_i)\frac{2}{3}\Delta x.\end{aligned}\tag{A.1}$$

For $i=j+1$

$$\begin{aligned}\int_{x_{i-1}}^{x_{i+1}} \chi_{\{u>0\}}\varphi_i\varphi_j dx &= \int_{x_{i-1}}^{x_i} \chi_{\{u>0\}}(u(x))\frac{1}{\Delta x}(x-x_{i-1})\frac{-1}{\Delta x}(x-x_{i-1})+1 dx \\ &= \int_{x_{i-1}}^{x_i} \tilde{\chi}(a_i)\left(-\frac{1}{\Delta x^2}(x-x_{i-1})^2\right)+\frac{1}{\Delta x}(x-x_{i-1})dx \\ &= \left[\tilde{\chi}(a_i)\left(-\frac{1}{3\Delta x^2}(x-x_{i-1})^3\right)+\frac{1}{2\Delta x}(x-x_{i-1})^2\right]_0^{\Delta x} \\ &= \tilde{\chi}(a_i)\frac{1}{6}\Delta x.\end{aligned} \tag{A.2}$$

Then the first term is

$$\int_{x_{i-1}}^{x_{i+1}} \chi_{\{u>0\}}\varphi_i\varphi_j dx = \begin{cases}\tilde{\chi}(a_i)\frac{4}{6}\Delta x & \text{if } i=j, \\ \tilde{\chi}(a_i)\frac{1}{6}\Delta x & \text{if } |i-j|=1, \\ 0 & \text{otherwise.}\end{cases} \tag{A.3}$$

Now, the second term if i=j is

$$\begin{aligned}\int_{x_{i-1}}^{x_{i+1}} (\varphi_x)_i(\varphi_x)_j dx &= \int_{x_{i-1}}^{x_i}\left(\frac{1}{\Delta x}\,\frac{1}{\Delta x}\right)dx+\int_{x_i}^{x_{i+1}}\left(\frac{-1}{\Delta x}\right)\left(\frac{-1}{\Delta x}\right)dx \\ &= \left[\frac{1}{\Delta x^2}\,x\right]_0^{\Delta x}+\left[\frac{1}{\Delta x^2}\,x\right]_0^{\Delta x} \\ &= \frac{2}{\Delta x}.\end{aligned} \tag{A.4}$$

For $i = j+1$

$$\begin{aligned}\int_{x_{i-1}}^{x_{i+1}}(\varphi_x)_i(\varphi_x)_j dx &= \int_{x_{i-1}}^{x_i}\frac{1}{\Delta x}\left(\frac{-1}{\Delta x}\right)dx \\ &= \left[\frac{-1}{\Delta x^2}x\right]_0^{\Delta x} \\ &= \frac{-1}{\Delta x}.\end{aligned} \tag{A.5}$$

Then the second term is

$$\int_{x_{i-1}}^{x_{i+1}}(\varphi_x)_i(\varphi_x)_j dx = \begin{cases}\dfrac{2}{\Delta x} & \text{if } i=j, \\ \dfrac{-1}{\Delta x} & \text{if } |i-j|=1, \\ 0 & \text{otherwise.}\end{cases} \tag{A.6}$$

Before we go to the third term we rewrite our basis function

$$\varphi_i(x) = \begin{cases}\dfrac{1}{\Delta x}x - i + 1 & x_{i-1} \le x \le x_i, \\ \dfrac{-1}{\Delta x}x + j + 1 & x_i \le x \le x_{i+1}, \\ 0, & \text{otherwise.}\end{cases}$$

We change the third term into column matrix if $i = j$

$$\begin{aligned}&\int_\Omega (\chi^\varepsilon)'(\sum_{i=0}^{N} a_i\varphi_i)\varphi_j dx = \\ &\int_{x_{i-1}}^{x_i}(\chi^\varepsilon)'(A_i(x))\left(\frac{1}{\Delta x}x - i + 1\right)dx + \int_{x_i}^{x_{i+1}}(\chi^\varepsilon)'(A_i(x))\left(\frac{-1}{\Delta x}x + i + 1\right)dx,\end{aligned} \tag{A.7}$$

where $A_i(x) = \dfrac{a_i - a_{i-1}}{\Delta x}(x - x_{i-1}) + a_i$ or $A_i(x) = \dfrac{a_{i+1} - a_i}{\Delta x}(x - x_i) + a_i$ according to the interval. We define x_i^0 and x_i^ε where $A_i(x_i^0) = 0$ and $A_i(x_i^\varepsilon) = \varepsilon$. We use linear interpolation to obtain x_i^0 and x_i^ε. For example we choose the interval between $[x_i, x_{i+1}]$

$$
\begin{aligned}
x_i^0 &= x_i - \frac{u_{i+1} + ui}{\Delta x} u_i, \\
x_i^\varepsilon &= x_i - \frac{u_{i+1} - u_i}{\Delta x} (u_i - \varepsilon),
\end{aligned}
\tag{A.8}
$$

Next, we define new space variables p and q and few cases as

$$
\begin{cases}
p_i = x_i, \quad q_i = x_{i+1} & \text{if } x_i^\varepsilon \le x_i \text{ and } x_{i+1} \le x_i^0, \\
p_i = x_i, \quad q_i = x_i^0 & \text{if } x_i^\varepsilon \le x_i \text{ and } x_i^0 \le x_{i+1}, \\
p_i = x_i^\varepsilon, \quad q_i = x_i^0 & \text{if } x_i \le x_i^\varepsilon \text{ and } x_i^0 \le x_{i+1}, \\
p_i = x_i^\varepsilon, \quad q_i = x_{i+1} & \text{if } x_i \le x_i^\varepsilon \text{ and } x_{i+1} \le x_i^0. \\
p_i = q_i & \text{otherwise}
\end{cases}
\tag{A.9}
$$

Rewrite (A.7)

$$
\begin{aligned}
&\int_{x_{i-1}}^{x_i} (\chi^\varepsilon)'(A_i(x)) \left(\frac{1}{\Delta x} x - i + 1 \right) dx + \int_{x_i}^{x_{i+1}} (\chi^\varepsilon)'(A_i(x)) \left(\frac{-1}{\Delta x} x + i + 1 \right) dx \\
&= \int_{p_{i-1}}^{q_{i-1}} \frac{1}{\varepsilon} \left(\frac{1}{\Delta x} x - i + 1 \right) dx + \int_{p_i}^{q_i} \frac{1}{\varepsilon} \left(\frac{-1}{\Delta x} x + i + 1 \right) dx \\
&= \frac{1}{\varepsilon} \left[\frac{x^2}{2\Delta x} - (i-1)x \right]_{p_{i-1}}^{q_{i-1}} + \frac{1}{\varepsilon} \left[\frac{-x^2}{2\Delta x} + (i+1)x \right]_{p_i}^{q_i} \\
&= \frac{1}{\varepsilon} \left(\frac{1}{2\Delta x} (q_{i-1}^2 - p_{i-1}^2 - q_i^2 + p_i^2) + (i-1)(q_{i-1} - p_{i-1}) + (i+1)(q_i - p_i) \right)
\end{aligned}
\tag{A.10}
$$

Acknowledgement

I would like to express my gratitude to my supervisor Prof. Seiro Omata who gave me guidance and support during my study. He also gave me his care to increase my knowledge in math.

My deep gratitude to Yoshiho Akagawa and Norbert Pozar for their patience while helping me during my study. A lot of things they shared to me. I indebted to them. My gratitude to my lab mate Alvi, Vita, Tris, and Giang for their assistance, discussion and encouragement.

I also express my gratitude to Indonesian Government (DIKTI) for their support for my study in Kanazawa University. At last but not the least, thank you to my family for their endless supports.

Parts of this dissertation are from an article with title "Numerical methods for 1-D hyperbolic-type problems with free boundary". This article was submitted to Science Reports Kanazawa University.

Bibliography

[1] E. Ginder, K. Svadlenka, *A variational approach to a constrained hyperbolic free boundary problem,* Nonlinear Analysis 71 (2009) e1527-e1537

[2] H. Imai, K. Kikuchi, K. Nakane, S. Omata, T. Tachikawa, *A numerical approach to the Asymptotic Behavior of Solution of a one-dimensional free boundary problem of hyperbolic type,* Japan J. of Ind. and Appl. Math. 18 (2001), 43 - 58.

[3] K. Ito, M. Kazama, H. Nakagawa, K. Svadlenka, *Numerical solution of a volume-constrained free boundary problem by the discrete Morse flow method,* Gakuto International Series, Mathematical Sciences and Application 29 (2008), 383-398.

[4] K. Kikuchi, S. Omata, *A free boundary problem for a one dimensional hyperbolic equation, Adv. Math. Sci. Appl. 9 (1999), 775 - 786*

[5] S. Omata, *A numerical treatment of film motion with free boundary,* Adv. Math. Sci. Appl. 14 (2004), 129 - 137.

[6] S. Omata, Norbert Pozar, *Private Discussion,* 2014.

[7] T. Yamazaki, S. Omata, K. Svadlenka, K. Ohara, *Construction of approximate solution to a hyperbolic free boundary problem with volume constraint and its numerical computation,* Adv. Math. Sci. Appl. 16/1 (2006), 57-67.

[8] T. Yamazaki, S. Omata, M. Nagayama, *Numerical simulation of motion of a bubble restrained to water surface,* Publications of The Research Institute for Mathematical Sciences, Kyoto University, proceedings of symposia No. 1522 (2006), 111-119